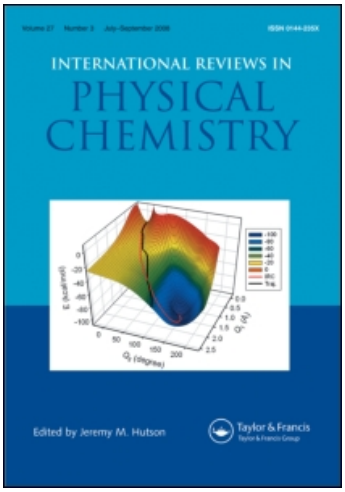

International Reviews in Physical Chemistry
Publication details, including instructions for authors and subscription information:
http://www.informaworld.com/smpp/title~content=t713724383

Theory of chemical bonding based on the atom-homogeneous electron gas system

Todd J. Raeker[a]; Andrew E. Depristo[a]
[a] Department of Chemistry and Ames Laboratory-U.S.D.O.E., Iowa State University, Ames, Iowa, USA

To cite this Article Raeker, Todd J. and Depristo, Andrew E.(1991) 'Theory of chemical bonding based on the atom-homogeneous electron gas system', International Reviews in Physical Chemistry, 10: 1, 1 — 54
To link to this Article: DOI: 10.1080/01442359109353253
URL: http://dx.doi.org/10.1080/01442359109353253

INTERNATIONAL REVIEWS IN PHYSICAL CHEMISTRY, 1991, VOL. 10, NO. 1, 1–54

Theory of chemical bonding based on the atom–homogeneous electron gas system

by TODD J. RAEKER and ANDREW E. DEPRISTO
Department of Chemistry and Ames Laboratory-U.S.D.O.E.,
Iowa State University, Ames, Iowa 50011, U.S.A.

We review recent developments in the theory of chemical bonding based upon replacement of an N-atom system by N individual systems each consisting of an atom embedded in a homogeneous electron gas. These theories include the corrected effective medium and effective-medium-based methods, which are either first principle or semi-empirical, as well as the embedded atom and related methods (e.g. the 'glue' and Finnis–Sinclair methods), which are totally empirical. These methods can provide an accurate description of metal–metal interactions for simple or transition metals with weak d bonding, including homogeneous and heterogeneous systems. They also can describe the binding of non-metallic atoms to metals. A number of these methods are efficient enough computationally to be used in molecular dynamics and/or Monte Carlo simulations of systems with many thousands of atoms.

1. Introduction

It is a formidable quantum mechanical problem to determine the energies and forces in multi-atom systems. For metals, the difficulty is increased because of the strongly delocalized nature of the electrons. For heavy elements, the problem is amplified by the large number of electrons (Salahub and Zerner 1989).

In this review, we present recent theories based upon the density functional formalism which are specifically designed to describe systems containing many metal atoms. Some of these theories have also been shown to be applicable to non-metal atoms and small systems. The central idea of all these methods is the replacement of a real N-atom system with many effective systems, each of which is one of the atoms embedded in jellium.† Since the atom-in-jellium forms the effective system while the jellium is the effective medium, one could label these as effective medium (EM) theories. Alternatively, one could focus on embedding the atom in jellium and label these embedded-atom methods (EAM). However, both these names now denote a particular form of these theories, not the general theoretical approach. Thus, throughout this review, we refer to the general theoretical methods as effective-medium type.

The concepts in effective-medium-type theories may seem foreign to chemists, who are familiar with the language of orbitals and their energies rather than embedding energies, electron density and its inhomogeneity. The detailed exposition of theoretical

† Jellium is a three-dimensional infinite homogeneous electron gas with a uniform compensating positive density. Upon embedding an atom in jellium, the electron density becomes inhomogeneous. The embedding energy is the difference between the atom–jellium and isolated atom and jellium systems.

methods in sections 2 and 3 allows for a global view of the effective-medium type approaches with considerable study and effort. In order to induce the reader into this effort, we provide an overview here, with an emphasis on qualitative understanding of the effective medium type concepts and methods.

Label the atoms by $\{A_i, i=1,\ldots,N\}$ where the A_i can be any type of atom. The interaction energy in the N-atom system, $\Delta E(\{A_i\})$, is written as

$$\Delta E(\{A_i\}) = \sum \Delta E_J(A_i; n_i) + \text{corrections}. \tag{1.1}$$

Here $\Delta E_J(A_i; n_i)$ is the embedding energy of A_i in jellium with electron density n_i; the summation extends over all N-atoms. The choice of the jellium densities and the form of the corrections distinguish the various theories based upon equation (1.1). Before considering these in detail, we make a few general points:

(*a*) the embedding energies are functions only of the identity of the atom and the electron density, and can be calculated and tabulated once and for all;

(*b*) the corrections take into account the differences between the more localized electron density and nuclear charges in the real N-atom system as compared to the atom-in-jellium systems.

Because of the second point, a fully self-consistent solution of equation (1.1) would require more work than a self-consistent solution of the original N-atom system. Hence, effective-medium-type-based theories are inherently not self-consistent. Instead, in these methods, one expects that the corrections are relatively small. Equation (1.1) should be looked at as a perturbation-theory expression in which a reference state of the atom-in-jellium systems is used rather than the standard reference of the vacuum. We do want to emphasize that the non-empirical theories based upon equation (1.1) used atoms and their densities to determine the jellium electron density; the jellium is really only used to translate an electron density into an energy via the embedding function.

Theories based upon this idea cover a wide spectrum. The most sophisticated and time-consuming computationally involve writing the corrections explicitly:

$$\Delta E(\{A_i\}) = \sum \Delta E_J(A_i; n_i) + \Delta V_c + \Delta G(\{A_i\}). \tag{1.2}$$

The embedding energies are taken from the SCF-LD calculations (Puska *et al.* 1981, Puska 1988) or determined from information on homonuclear diatomic and bulk systems of atom A_i. ΔV_c is the difference in the Coulombic energy between the N-atom system and the N atom-in-jellium systems. ΔG is a similar difference but for the sum of the kinetic, exchange, and correlation energies. The two methods which use equation (1.2) are the corrected effective medium (CEM) theory (Kress and DePristo 1988, Kress *et al.* 1989, Raeker and DePristo 1989) and the effective medium theory in its most recent version due to Nørskov and co-workers (Jacobson *et al.* 1987, Jacobson 1988). The former uses atomic Hartree–Fock (HF) densities and direct evaluation of both the Coulomb integrals and the kinetic-exchange-correlation integral. It is applicable to large and small systems. The latter employs atom-induced densities in the atom-in-jellium system and approximates ΔV_c and ΔG in a manner appropriate for extended systems. The former is more computationally demanding than the latter.

The physical factors contributing to the correction, ΔV_c and ΔG, can be identified. The first is the difference in homogeneity between the electron density distributions in the real and atom-in-jellium systems. The second is the difference between the uniform positive background in the jellium and the point nuclear charges in the real system. The third is the difference in spin-polarization between the real system and the unpolarized atom-in-jellium one.

Historically, both the CEM and EM theories were developed in the form of an active atom embedded in an inert metallic host (Kress and DePristo 1987, Nørskov and Lang 1980, Stott and Zaremba 1980). We ignore these theories throughout this review (with the exception of a brief discussion of their application to atomic chemisorption in section 4), always referring to CEM and EM as the form in which all atoms are embedded in jellium. The interested reader may consult a number of earlier reviews including some rather recent ones (Nørskov and Besenbacher 1987, Lundqvist *et al.* 1987, McMullen *et al.* 1989).

A less sophisticated and semi-empirical theory results from neglecting the last term in equation (1.2) and using empirical embedding functions:

$$\Delta E(\{A_i\}) = \sum \Delta F_J(A_i; n_i) + \Delta V_c. \tag{1.3}$$

The embedding functions, ΔF_J, are determined from information on homonuclear diatomic and/or bulk systems of atom A_i. ΔV_c is still the difference in the Coulombic energy between the N-atom system and the N atom-in-jellium systems. The method which uses equation (1.3) is the molecular dynamics/Monte Carlo corrected effective-medium N-body theory (MD/MC-CEM) (Stave *et al.* 1990). It is so named since the energies and forces based upon equation (1.3) can be evaluated fast enough to perform MD and MC simulations on large systems (Sanders *et al.* 1990). The simple expression in equation (1.3) is less accurate than the full CEM theory, especially for cases in which there are inhomogeneous electron densities. In those cases, the neglect of the ΔG term leads to substantial inaccuracies in geometrical predictions.

It is worthwhile to note that equation (1.3) still uses atomic HF densities and direct evaluation of the Coulomb integrals. The jellium densities and Coulomb energies are non-empirical, and the embedding functions are not dependent upon the environment. Hence equation (1.3) can be used to predict the behaviour of heterogeneous systems once the embedding functions have been determined from properties of the homogeneous systems.

The simplest theories are the purely empirical embedded-atom method (Daw and Baskes 1984, Daw 1989), 'glue' model (Ercolessi *et al.* 1986, 1987a, 1987b, 1988) and Finnis–Sinclair method (Finnis and Sinclair 1984, Finnis *et al.* 1988). These remove the connection to any calculated atomic densities, simply by using arbitrary forms for an electron density function in the case of the EAM and Finnis–Sinclair methods; in the 'glue' model, an effective coordination function is employed instead of an electron density function. All these methods replace the calculated Coulomb integrals with empirical two-body potentials, leading to

$$\Delta E(\{A_i\}) = \sum \Delta f_J(A_i; n_i) + \sum_i \sum_{j \neq i} V_2(i,j). \tag{1.4}$$

The electron density functions, embedding functions and pair potentials are determined by fitting to certain types of experimental data. In these empirical theories, the two-body potentials must be determined for all types of atoms in a heterogeneous system. Hence one cannot generally predict the behaviour of heterogeneous systems from homogeneous ones. Instead, one uses some properties of the heterogeneous systems to predict other properties. Thus these methods are best considered as reasonably sophisticated representations of many-body potentials involving metallic systems. It is unlikely that such methods can be useful in small systems without additional empirical constructs.

The range of these theories has led to some confusion in the literature, especially regarding the relationships between the semi-empirical EM theory of Nørskov and

co-workers and the empirical EAM, 'glue' and Finnis–Sinclair methods. The above qualitative presentation and the details presented later in this review demonstrate that effective-medium-type theories range from (non-self-consistent) first principle to semi-empirical to empirical methods. This is similar to the situation in conventional chemical approaches except that self-consistent *ab initio* or density-functional theories are absent, of course. We should also emphasize that effective-medium-type methods do not provide any information on electronic wavefunctions, just interaction energies for specific nuclear geometries. Thus they are more limited than wavefunction approximations but can also be substantially more accurate and much more efficient computationally.

Effective-medium-type theories are also closely related to the electron-gas theory (Gordon and Kim 1972, Kim and Gordon 1974, Waldman and Gordon 1979, Muhlhausen and Gordon 1981). Indeed, the effective-medium-type theory can be thought of as simply the electron-gas theory using a different reference system, namely the atom-in-jellium. This greatly increases the accuracy of electron-gas methods in the same way that pertubation theory increases in accuracy for any problem as the zeroth-order model improves. This type of reasoning may be useful for chemists familiar with the Gordon–Kim applications, and especially with the inability of the electron gas to describe chemical bonding. Such inadequacies do not arise in the effective-medium-type methods because the atom-in-jellium system contains many of the features in chemical bonding, especially for ionic bonds. We do not want to overemphasize the electron-gas theory since it is only the corrections in effective-medium-type methods that are provided by the electron gas, and even these can be found in other ways. The central feature of effective-medium-type theories is the atom embedded in jellium.

Our presentation will be logical rather than chronological, completely ignoring the early less general theories. We start by considering the typical low-symmetry systems of any types of atoms that are found in chemistry. Later, we will implement various translational symmetries to provide treatments of surfaces and solids that are more typically found in physics. In addition, we will derive the various methods in a logical and hierarchical manner, starting with the most sophisticated and direct treatment of the correction terms, and leading to the most empirical forms, basically useful for the representation of many-body potential-energy surfaces.

As in any review, we have tried to provide an accurate assessment of the current literature. Because of the simplicity of some of the interaction energy models presented herein, a great number of very short papers have been published consisting of a straightforward application; the main conclusion is invariably that the theory and experiment agree. We will not burden the reader with exhaustive description of such applications. Instead, we try to indicate the overall nature of the field, stressing the concepts, capabilities and even the incapabilities.

2. First-principle and semi-empirical effective-medium-type theories

In this section, we develop the effective-medium-type theories, focusing on the CEM method which has been applied to systems with an arbitrary number of particles and geometry (Kress and DePristo 1988, Kress *et al.* 1989, Raeker and DePristo 1989, Stave *et al.* 1990). We also present the newest EM method (Jacobson *et al.* 1987, Jacobson 1988) which is also applicable to an arbitrary number of particles and which was derived independently around the same time. These two methods are equivalent in their fundamental formalism but differ in implementation.

An important point is that the CEM method is a non-self-consistent first-principles approach when used with the SCF-LD embedding energies of atoms in jellium (Puska *et al.* 1981, M. J. Puska 1988, private communication) and the atomic HF densities (Clementi 1965, Bagus *et al.* 1972). There are no parameters to determine from experimental data. Alternatively, with an embedding function determined from experimental data, the CEM method becomes a semi-empirical method.

2.1. *Corrected effective medium theory*

The derivation follows that of Kress and DePristo (1988) to which the reader is referred for further details. As in section 1, we consider an N-body system consisting of atoms $\{A_i, i=1,\ldots,N\}$ where the A_i can be any type of atom. The nuclear positions are $\{\mathbf{R}_i\}$, nuclear charges are $\{Z_i\}$, and the electronic coordinates relative to each nuclear positions are $\{\mathbf{r}_i\}$. The spin-up, spin-down and total electron density around each atom are denoted by $n^+(A_i;\mathbf{r}_i)$, $n^-(A_i;\mathbf{r}_i)$ and $n(A_i;\mathbf{r}_i)$ respectively.

The desired quantity is the energy difference between the interacting and non-interacting systems of atoms, denoted by

$$\Delta E(\{A_i\}) = E(\sum A_i) - \sum E(A_i). \tag{2.1}$$

To evaluate this energy difference, we use the energy of each atom embedded into jellium (Puska *et al.* 1981, Puska 1988, private communication), defined by

$$\Delta E_J(A_i;n_i) = E(A_i+n_i) - E(n_i) - E(A_i) \tag{2.2}$$

Here $E(n_i)$ and $E(A_i+n_i)$ are respectively the energies of the jellium and of the jellium plus atom A_i system. (The notation in Kress and DePristo has an added subscript J on some total energy quantities, e.g. $E_J(A_i;n_i)$, which is not needed since the appearance of n_i always indicates jellium.) Elimination of the atom energy, $E(A_i)$, common to equations (2.1) and (2.2) leads to the first fundamental relationship of the CEM theory:

$$\Delta E(\{A_i\}) = \sum \Delta E_J(A_i;n_i) + E(\sum A_i) - \sum [E(A_i+n_i) - E(n_i)] \tag{2.3}$$

In equation (2.3), the first term on the right-hand side is the sum of the embedding energies for each atom in jellium of some (as yet unspecified) electron density n_i. These energies can be evaluated from SCF-LD calculations (Puska *et al.* 1981, Puska 1988, private communication) or from other, semi-empirical, methods as discussed in subsection 2.5. We will not distinguish between these two functions until then. The form of the remaining three terms in equation (2.3) and the choice of the densities n_i are addressed in the remainder of this subsection.

The energy is composed of Coulombic, kinetic, exchange and correlation parts. We denote this separation by

$$E(\{A_i\}) = V_c(\{A_i\}) + G(\{A_i\}), \tag{2.4}$$

where V_c is the Coulombic energy and G is the sum of the kinetic and exchange-correlation energies, T and E_{xc} respectively. Substitution of equation (2.4) into equation (2.3) yields the second fundamental relationship of CEM theory,

$$\Delta E(\{A_i\}) = \sum \Delta E_J(A_i;n_i) + \Delta V_c + \Delta G(\{A_i\}) \tag{2.5 a}$$

where

$$\Delta G(\{A_i\}) = G(\sum A_i) - \sum [G(A_i+n_i) - G(n_i)] \tag{2.5 b}$$

Equation (2.5 *a*) expresses the stabilization energy of the N-atom cluster as a total of three terms.

(*a*) The sum of the embedding energies for the atoms in jellium.
(*b*) The difference in the Coulombic energy between the real system and all the atoms in jellium.
(*c*) The difference in the sum of the kinetic, exchange, and correlation energies between the real system and all the separated atoms in jellium.

This decomposition is useful since the physical factors contributing to ΔV_c and ΔG can be identified.

For ΔV_c, there are two physical effects. The first is the difference in homogeneity of the electron density distributions in the real and atom-in-jellium systems. The second is the difference between the uniform positive background in the jellium and the point nuclear charges in the real system. For ΔG, there are also two effects. The first, and most important, is again the difference in uniformity of the electron density distributions. The second is the (possible) difference in spin-polarization between the real system and the unpolarized atom-in-jellium one.

Since self-consistent evaluation of equation (2.5 *a*) would be as difficult as evaluation of the original equation (2.1), progress requires an approximate evaluation of equation (2.5 *a*) based upon some *Ansatz* about the relationship between the electron density of the N-atom system and that of the N individual atoms. (A similar *Ansatz* must be applied to the A–J system *versus* the A and J separately.) The fundamental assumption is that the electron density at any point in space, $\mathbf{r}$, is the sum of the spin-densities from each atom:

$$n^+(\mathbf{r}) = \sum n^+(\mathrm{A}_i; \mathbf{r} - \mathbf{R}_i) \tag{2.6a}$$

$$n^-(\mathbf{r}) = \sum n^-(\mathrm{A}_i; \mathbf{r} - \mathbf{R}_i) \tag{2.6b}$$

It is important to note that the effects of electron inhomogeneity and spin-polarization do not vanish even within this superposition approximation. Indeed, since the difference in the energies of the real *versus* jellium systems is calculated, we expect lower sensitivity to the use of accurate electron densities than the direct calculation of energetics in either system by itself, assuming of course that the proper electron density in the jellium is used. In other words, a self-consistent calculation is employed via the $\Delta E_J(\mathrm{A}_i; n_i)$ and only the corrections due to inhomogeneity and spin-polarization of the electron and positive charge distribution are calculated non-self-consistently. More rigorously, one may resort to density-functional theory to demonstrate that a first-order error in the electron density leads to a second-order error in the energy (Nørskov and Lang 1980, Stott and Zaremba 1980, Nørskov and Besenbacher 1987, Lundqvist *et al.* 1987, McMullen *et al.* 1988).

First consider the Coulombic energies. Since the additive electron density approximation is assumed to hold for each atom in the jellium also, the electrostatic interaction in the jellium system vanishes. The difference in Coulombic energies is then given by that of the real system only:

$$\Delta V_c = \frac{1}{2} \sum_i \sum_{j \neq i} V_c(i,j) \tag{2.7a}$$

$$V_c(i,j) = \int [n(\mathrm{A}_i; \mathbf{r}_1 - \mathbf{R}_i) - Z_i \delta(\mathbf{r}_1 - \mathbf{R}_i)] r_{12}^{-1} [n(\mathrm{A}_i; \mathbf{r}_2 - \mathbf{R}_j) - Z_j \delta(\mathbf{r}_2 - \mathbf{R}_j)] \, \mathrm{d}\mathbf{r}_1 \, \mathrm{d}\mathbf{r}_2. \tag{2.7b}$$

These electron–electron and electron–nuclear integrals can be evaluated by standard methods (Huzinaga 1967).

There are three remaining problems. First, accurate electron spin-density functionals must be used for the kinetic, exchange and correlation energies. Second, a proper choice of the jellium electron density must be determined. Third, the calculation of the corrections involves a multi-centre three-dimensional integration over the functionals of the electron density, which must be performed precisely and efficiently. The first and second points are addressed in this subsection, while the third is relegated to subsection D which also includes details of the CEM calculations.

The function G is written as

$$G=\int [\tau(n^+(\mathbf{r}))+\tau(n^-(\mathbf{r}))+\epsilon_{xc}(n^+(\mathbf{r}),n^-(\mathbf{r}))]\,d\mathbf{r}. \tag{2.8}$$

The functions for the exchange-correlation energy, $\epsilon_{xc}(n)$, must be the same as used in the SCF-LD calculations of the atom-in-jellium system or else the atomic energies cannot be eliminated between equation (2.1) and (2.2). The SCF-LD calculations employed the local Dirac exchange (Dirac 1930) and local Gunnarsson–Lundqvist correlation functionals (Gunnarsson and Lundqvist 1976).

Since the SCF-LD results used the exact kinetic energy within the Kohn–Sham formalism, an accurate Pade approximant representation of the full gradient expansion is used (DePristo and Kress 1987). This provides the kinetic energy density function for either up or down electron spin-density symbolized here by $n^{\pm}(\mathbf{r})$:

$$\tau(n^{\pm}(\mathbf{r}))=\tau_0(n^{\pm}(\mathbf{r}))\frac{(1+0{\cdot}95x+14{\cdot}28111x^2-19{\cdot}57962x^3+26{\cdot}64777x^4)}{(1-0{\cdot}05x+9{\cdot}99802x^2+2{\cdot}96085x^3)} \tag{2.9a}$$

$$\tau_0(n^{\pm}(\mathbf{r}))=\frac{3}{10}(6\pi^2)^{2/3}n^{\pm}(\mathbf{r})^{5/3} \tag{2.9b}$$

$$x=\frac{5}{108}(6\pi^2)^{-2/3}\frac{|\nabla n^{\pm}(\mathbf{r})|^2}{n^{\pm}(\mathbf{r})^{8/3}}. \tag{2.9c}$$

The variable x is the ratio of the second-order gradient term to the zeroth-order term. This functional reproduces the kinetic energies of atoms quite accurately. However, it becomes the Weizacker form,

$$\tau(n^{\pm}(\mathbf{r}))\rightarrow|\nabla n^{\pm}(\mathbf{r})|^2/8n^{\pm}(\mathbf{r})$$

as $x\rightarrow\infty$, and this may overestimate the kinetic energy for small densities and large gradients. Such an overestimate will be significant for weakly interacting systems only. In these cases, one can simply use $\tau_0(n^{\pm}(\mathbf{r}))$.

The question of exchange-correlation functionals is worthwhile to discuss a little more since more accurate exchange (Becke 1986, Ghosh and Parr 1986, Perdew and Yue 1986, DePristo and Kress 1988) and correlation (Perdew 1986) energy functionals are available. We have used some of these functionals when the SCF-LD embedding energies have been replaced by an empirically constructed form as explained in subsection 2.5. We have found that this is not particularly important for the interaction energies, especially compared to a number of more severe problems with choice of the atomic occupations as described in subsection 2.4.

The determination of the jellium electron density is considered next. Since the non-self-consistent part of the CEM formalism is expected to be less accurate than the self-

consistent part, we minimize the $|\Delta G|$ term in the former† with respect to the $\{n_i\}$. Since G is a complicated functional of both the electron spin-densities and their gradients, an analytic minimization of $|\Delta G|$ is not possible, and a numerical minimization does not provide insight into the proper choice of the jellium densities. However, examining the variation of the sum of the leading terms, which are local kinetic-exchange energy, with n^+ shows that the integrand can be approximated quite closely by a quadratic in n^+ (Kress and DePristo 1987). Within this quadratic approximation for the functional in both $n+$ and $n-$, we have

$$\Delta G \approx C \sum_i \sum_{j \neq i} \int \{n^+(\mathrm{A}_i; \mathbf{r}-\mathbf{R}_i) n^+(\mathrm{A}_j; \mathbf{r}-\mathbf{R}_j) + n^-(\mathrm{A}_i; \mathbf{r}-\mathbf{R}_i) n^-(\mathrm{A}_j; \mathbf{r}-\mathbf{R}_j)\} \, \mathrm{d}\mathbf{r}$$

$$-2C \sum_i \int \{n^+(\mathrm{A}_i; \mathbf{r}-\mathbf{R}_i) n_i^+ + n^-(\mathrm{A}_i; \mathbf{r}-\mathbf{R}_i) n_i^-\} \, \mathrm{d}\mathbf{r}_i, \tag{2.10a}$$

where C is the coefficient of the quadratic fit. Since the SCF-LD jellium uses an unpolarized electron gas, $n_i^+ = n_i^- = n_i/2$ in equation (2.10*a*), yielding

$$\Delta G \approx C \sum_i \sum_{j \neq i} \int \{n^+(\mathrm{A}_i; \mathbf{r}-\mathbf{R}_i) n^+(\mathrm{A}_j; \mathbf{r}-\mathbf{R}_j) + n^-(\mathrm{A}_i; \mathbf{r}-\mathbf{R}_i) n^-(\mathrm{A}_j; \mathbf{r}-\mathbf{R}_j)\} \, \mathrm{d}\mathbf{r}$$

$$-C \sum_i Z_i n_i. \tag{2.10b}$$

Minimization of $|\Delta G|$ in equation (2.10*b*) leads to solutions for n_i which are *independent* of the coefficient C. The most symmetric solution is

$$n_i = \sum_{j \neq i} Z_i^{-1} \int \{n^+(\mathrm{A}_i; \mathbf{r}-\mathbf{R}_i) n^+(\mathrm{A}_j; \mathbf{r}-\mathbf{R}_j) + n^-(\mathrm{A}_i; \mathbf{r}-\mathbf{R}_i) n^-(\mathrm{A}_j; \mathbf{r}-\mathbf{r}_j)\} \, \mathrm{d}\mathbf{r} \tag{2.11a}$$

This possesses a number of reasonable physical properties. First, the jellium electron density on atom A_i due to atom A_j is proportional to the electron spin-density of A_j averaged over atom A_i with the weight function equal to the (normalized) electron spin-density of A_i. Since the 'size' of atom A_i can be characterized by the atomic electron spin-density, such an average makes good physical sense. Second, for the case of *spin-unpolarized* atoms, n_i becomes

$$n_i = \frac{1}{2} \sum_{j \neq i} Z_i^{-1} \int n(\mathrm{A}_i; \mathbf{r}-\mathbf{R}_i) n(\mathrm{A}_j; \mathbf{r}-\mathbf{R}_j) \, \mathrm{d}\mathbf{r}. \tag{2.11b}$$

This is half of the total electron density average because of a division of electron density between the two atoms, an effect which is analogous to dividing up a pair potential V_{ij}, into $\frac{1}{2}V_{ij} + \frac{1}{2}V_{ji}$ and which thus eliminates overcounting of embedding energies. (Note that for a given pair of atoms, i and j, the electron density overlap contribution is equal on each atom but the electron density contribution is not, because of the inverse weighting by the atomic number.) Third, the integral in equation (2.11) is positive for all densities.

† It is not possible to minimize the term $\Delta V_c + \Delta G$, since the Coulombic energy can become so negative as to yield a negative value for the jellium density.

It is worthwhile to emphasize that the CEM energies are not invariant to arbitrary changes in n_i because the ΔG terms are not calculated self-consistently, and thus an optimal choice of n_i is important. However, small variations of n_i do not alter significantly the CEM energies because of a cancellation between the embedding energies and ΔG. The original functional is used in numerical calculations of ΔG and the approximation is only necessary to find an analytic choice for n_i.

2.2. *Periodic structures*

The theory in subsection 2.1 was applicable for arbitrary geometries and number of atoms. It is illustrative to incorporate translational periodicity directly for solids (Kress *et al.* 1989) and surfaces (Raeker and DePristo 1989).

First consider a system with full three-dimensional (3D) periodicity. Let the αth unit cell contain atoms $\{A_{\alpha k}, k=1, N_c\}$. The summation over '$i$' in equation (2.5 *a*) can then be written using equations (2.7) as a summation over unit cells times a summation over atoms in the unit cell:

$$\Delta E(\{A_i\}) = \sum_{\alpha} \sum_{k} \Delta E_J(A_{\alpha k}; n_{\alpha k}) + \frac{1}{2} \sum_{\alpha} \sum_{k} \sum_{\alpha'} \sum_{k'} \Delta V_c(\alpha k, \alpha' k') + \Delta G(\{A_{\alpha k}\}). \tag{2.12}$$

One part of ΔG contains a summation over the atom-in-jellium terms, see equation (2.5 *b*), which can easily be changed to a summation over unit cells and atoms in the cell. The only part which may be somewhat confusing is the term in $G(\Sigma A_i)$ that involves an integration over the functionals of the electron density of the entire system. However, the integral can be evaluated as many integrals over coordinate space closest to all the atoms in each unit cell:

$$G\left(\sum_{\alpha k} A_{\alpha k}\right) = \sum_{\alpha} G\left(\sum_{k} A_{\alpha k}\right)_{WS(\alpha)}. \tag{2.13}$$

The subscript WS(α) indicates that the integral is evaluated only over this restricted region of configuration space, the Wigner–Seitz cell of the αth unit cell.

Combining equations (2.12) and (2.13), and explicitly writing the summation over unit cells and atoms for the $G(A_i; n_i)$ terms in equation (2.5 *b*), yields the equation for 3D periodic structures:

$$\begin{aligned} \Delta E(\{A_i\})_{coh} = & \sum_{k} \Delta E_J(A_{\alpha k}; n_{\alpha k}) + \frac{1}{2} \sum_{k} \sum_{\alpha'} \sum_{k'} \Delta V_c(\alpha k, \alpha' k') \\ & + G\left(\sum_{k} A_{\alpha k}\right)_{WS(\alpha)} - \sum_{k} [G(A_{\alpha k}; n_{\alpha k}) - G(n_{\alpha k})]. \end{aligned} \tag{2.14}$$

In this equation, α refers to *any* unit cell, while α' extends over *all* cells including α. (The term with $\alpha' = \alpha$ and $k' = k$ in the Coulomb summation is not included, of course.) We have identified the value of $\Delta E/\Sigma_\alpha$ as the cohesive energy. This is the energy gained in formation of an infinite periodic structure with N_c atoms per unit cell from isolated atoms. Note how much more efficient equation (2.14) is than the original equation (2.12). The summations in the embedding and correction energies extend over the atoms in the unit cell, not over all atoms. The Coulomb summation involves only one summation over unit cells in order to incorporate intercellular Coulomb interactions. All of these terms can be evaluated quite efficiently.

Two-dimensional periodicity can be incorporated in much the same way. One simply recognizes that each unit cell in a particular layer is equivalent to every other cell in the same layer. This leads immediately to the result:

$$\Delta E([\mathrm{A}_i\})_\alpha = \sum_k \Delta E_J(\mathrm{A}_{\alpha k}; n_{\alpha k}) + \frac{1}{2}\sum_k \sum_{\alpha'} \sum_{k'} \Delta V_c(\alpha k, \alpha' k') + G\left(\sum_k \mathrm{A}_{\alpha k}\right)_{\mathrm{WS}(\alpha)} - \sum_k [G(\mathrm{A}_{\alpha k}; n_{\alpha k}) - G(n_{\alpha k})] \tag{2.15}$$

where ΔE_α is the interaction energy for the atoms in any unit cell in the αth layer. Two points are worthwhile mentioning. First, as α becomes a bulk layer, the energy in equation (2.15) coincides with that in equation (2.14). Second, equation (2.15) is applicable to adsorbates at any coverage since the summation over k and k' depends upon the layer indices α and α'.

The jellium densities for any atom in both the 2D and 3D periodic formulae are computed from the general expression in equation (2.11). Translational periodicity plays no role since there is only a single summation over the surrounding atoms. This summation is truncated when the overlaps become small, just as for the Coulomb integral contribution in equation (2.14) and (2.15).

2.3. *Effective-medium theory*

The EM theory has been presented in a number of lucid articles (Jacobson *et al.* 1987, Jacobson and Nørskov 1987, 1988, Stoltze *et al.* 1987, 1988) and a review (Jacobson 1988). A chemically-oriented article is the recent work dealing with the extension of the EM method to include dissociation of diatomic molecules on metal surfaces (Nørskov 1989). A complete discussion of the N-body theory is found in Jacobson *et al.* (1987). We refer the reader to these articles for details.

The starting point is again equation (2.5) which is not surprising since that is a general equation simply relating the full N-atom and N-atom-in-jellium systems. The difference between EM and CEM methods involves the determination of the jellium densities, the evaluation of ΔV_c and the calculation of $\Delta G(\{\mathrm{A}_i\})$. In other words, in the details.

First, the EM method uses the induced atomic electron densities from the SCF-LD calculation for the atom-in-jellium system rather than the HF atomic electron densities. Use of this induced electron density then leads to the idea of a neutrality sphere around each atom with radius s_i. The $\{n_i\}$ are chosen as the average electron densities of other atoms within this sphere.

Second, for the Coulomb integrals, the fundamental assumption is that the ith atom interacts with the electron density in the real system exactly as it interacts with jellium. The integrals are approximated as

$$\Delta V_c \approx -\alpha_i n_i + \Delta V_{\mathrm{AS}}, \tag{2.16}$$

$$\alpha_i = \int_{s_i} \Delta\phi(\mathbf{r})\,\mathrm{d}\mathbf{r}, \tag{2.17}$$

where $\Delta\phi$ is the atom-induced electrostatic potential and the integration extends only over the neutrality radius, s_i. The atomic sphere term, ΔV_{AS}, corrects for the fact that some parts of space are not counted while others are counted twice due to the use of a neutrality radius around each atom.

Combining equations (2.16) with (2.5 *a*) yields

$$\Delta E(\{A_i\}) = \sum \Delta E_{EM,i}(A_i; n_i) + \Delta V_{AS} + \Delta G(\{A_i\}) \tag{2.18 a}$$

where the new embedding functions are defined as

$$\Delta E_{EM,i}(A_i; n_i) = \Delta E_P(A_i; n_i) - \alpha_i n_i. \tag{2.18 b}$$

Furthermore, the term in ΔG is identified as the difference in the one-electron energies between the real and atom-in-jellium systems. (The SCF-LD embedding energies (Puska *et al.* 1981, Puska 1988, private communication) are referred to as ΔE_P to distinguish them from other embedding functions are described in subsection 2.5.)

In the EM theory, all atoms are spherically symmetric and unpolarized. Furthermore, the EM method requires explicit estimation of the one-electron energy differences whenever partly filled d shells occur. The reader interested in more details should consult the original papers.

2.4. *Details of the CEM theory*

The HF electron density and numerical integration are two important details in the CEM theory. The electron density of each atom is determined from the wavefunctions (Clementi 1965, Bagus *et al.* 1972). These are expressed in a basis of Slater-type orbitals. Since Slater orbitals are inconvenient for calculation of overlaps and Coulomb integrals, we have fitted the electron density in an even-tempered Gaussian basis (Schmidt and Ruedenberg 1979). The particular type of even-tempered spherical basis is $\{\exp(-\alpha\beta^{f(n)}r^2)\}$, and the non-spherical p type orbital basis is

$$\{x^2 \exp(-\alpha\beta^{f(n)}r^2), y^2 \exp(-\alpha\beta^{f(n)}r^2), z^2 \exp(-\alpha\beta^{f(n)}r^2)\}.$$

The function $f(n) = n^\delta$ and the constants are α, β and δ. There is nothing fundamental about this even-tempered Gaussian representation and any Gaussian basis could be used. For all atoms, the d shell is sphericalized and included in the spherical electron density. The only non-spherical electron density is of p type. The Gaussian basis allows for simple evaluations of the Coulomb and overlap integrals (Huzinaga 1976).

The evaluation of ΔG involves N three-dimensional single-centre integrals in $G(A_i; n_i)$ and one three-dimensional N-centre integral in $G(\Sigma A_i)$. The former can be easily evaluated using Gaussian integration schemes (Stroud and Secrest 1966, Abramowitz and Stegun 1972). The latter presents a rather difficult problem which is evaluated using the 'fuzzy' cell integration method of Becke (1988) and Delley (1990).

Consider the generic integral

$$I = \int F(\mathbf{r})\, d\mathbf{r} \tag{2.19}$$

which can be rewritten exactly as

$$I = \sum \int w_n(\mathbf{r}) F(\mathbf{r})\, d\mathbf{r} \tag{2.20}$$

under the restriction on the weight functions,

$$\sum w_n(\mathbf{r}) = 1. \tag{2.21}$$

These functions are chosen to be unity when $|\mathbf{r} - \mathbf{R}_n|$ is much smaller than $|\mathbf{r} - \mathbf{R}_j|$ with $j \neq n$, and to fall-off quickly to zero whenever this condition does not hold. The multi-centre three-dimensional integral in equation (2.19) is thereby transformed into many

single-centre three-dimensional integrals

$$I=\sum \int f_n(\mathbf{r})\,d\mathbf{r} \tag{2.22 a}$$

where

$$f_n(\mathbf{r})=w_n(\mathbf{r})F(\mathbf{r}). \tag{2.22 b}$$

In the limit that the w_n are step functions in the minimum distance, the f_n are discontinuous, which is poor for numerical integration. The clever idea was to define a set of $\{w_n\}$ which make the $\{f_n\}$ smooth and thus amenable to efficient numerical integration. The reader should consult the articles by Becke (1988) and Delley (1990) for further details.

In CEM, the calculation of all single-centre integrals such as $G(A_i; n_i)$ and equation (2.22 *a*) is accomplished by Gaussian quadrature of the Laguerre, Legendre and Chebyshev forms for the radial, polar and azimuthal integration (Abramowitz and Stegun 1972). The Laguerre integration uses the weights for associated Laguerre polynomials with $\alpha=3/2$ (Stroud and Secrest 1972). About 5000–10 000 points per centre have been found to yield ΔG accurate to better than 0·0001 eV.

The next detail involves evaluation of the integrands for the kinetic-exchange-correlation integrals, which require the atomic densities and gradients at a large number of spatial points, $\geqslant 5\,000\,N$. Direct evaluation of these densities and gradients using either Slater or Gaussian basis sets is much too slow. Instead, we have evaluated and stored the radial parts of the spherical, p_x, p_y and p_z type densities and their associated radial derivatives on a large evenly spaced grid from $r=10^{-8}$ atomic units to some large value, r_m. (The value of r_m is chosen such that $r_m^2 n(r_m)$ is smaller than some cut-off value, with 10^{-5} used at present.) Values at other points are found from linear interpolation, which is very fast since the interval can be found without a search on this evenly spaced grid.

The final detail about the electron density involves the occupation of each atomic orbital in the HF atom. While this is fixed for each atomic shell, there is no energy difference associated with certain variations of occupations within an atomic shell, so $3p_x$, $3p_y$ or $3p_z$ can be filled with either an up-spin or down-spin electron in Al. Formation of a molecule will be quite dependent upon the particular filling since CEM is not a self-consistent theory and thus does not allow the occupations to vary during the calculation. An additional complexity occurs since it is really the difference between the atoms in the N-atom system and the N atom-in-jellium systems that is calculated. The spin-polarization of the former should reflect the spin-polarization in the N-atom system and not necessarily that of the isolated atoms.

It is easy to understand the above problem by example. For the O_2 molecule with the z axis coincident with the bond axis, a number of different occupations are possible, with three listed below:

Atom 1 (Atom 2)	1s	2s	$2p_x$	$2p_y$	$2p_z$
O	+1, −1	+1, −1	+1, −1	+1, 0	+1, 0
(O)	+1, −1	+1, −1	+1, −1	0, −1	0, −1
O	+1, −1	+1, −1	+1, −1	+1/2, −1/2	+1/2, −1/2
(O)	+1, −1	+1, −1	+1, −1	+1/2, −1/2	+1/2, −1/2
O	+1, −1	+1, −1	+2/3, −2/3	+2/3, −2/3	+2/3, −2/3
(O)	+1, −1	+1, −1	+2/3, −2/3	+2/3, −2/3	+2/3, −2/3

The first occupation is analogous to a valence bond configuration with spin-pairing in the molecule for both p_y and p_z orbitals, forming pi and sigma bonds. The second configuration is analogous to a molecular-orbital description of the same spin-pairing. The third configuration yields a spherical unpolarized description of the O atoms in the O_2 molecule. Calculations (Kress and DePristo 1988) indicate that either unpolarized configuration is adequate. However, this is only a preliminary result and the subject of spin-polarization and directional bonding in the CEM theory must be considered further in the future. Applications have not considered strong directionally bonded systems and indeed have used a full ns^2 configuration for all transition metals along with sphericalization of the d shell.

2.5. *CEM embedding functions:* ΔE_J

All aspects of the CEM theory have now been presented except for the embedding functions. The non-empirical choice uses the results of SCF-LD calculations, which are available for a number of atoms (Puska *et al.* 1981, Puska 1988, private communication), and will be referred to with the subscript P in place of the J to indicate the particular type of solution, $\Delta E_P(A;n)$.

We show all the available $\Delta E_P(A;n)$ functions in figure 1. The intercept at zero electron density is the negative of the electron affinity of atom A, and is added to the SCF-LD values (Hotop and Lineberger 1975). For an atom with positive electron affinity this function has the characteristic shape shown in figure 2 for N and F. The small decrease of $\Delta E_P(A;n)$ with increasing electron density at low electron density is due to reorganization of the originally uniform electron density in jellium around the atom. The large increase in energy at high electron density is due to the kinetic energy repulsion between the electrons of the atom and those of the jellium.

The troublesome behaviour when using $\Delta E_P(A;n)$ to model the interactions in systems composed of atoms is the intercept at $-EA$. This feature is a direct result of the vanishing of the work function for jellium in the zero electron density limit, and corresponds to an electron transfer from jellium to the embedded atom. This also indicates a clear breakdown of the electron density superposition approximation. For real non-interacting systems, the electron density n will vanish via equations (2.11 *a*) or (2.11 *b*), thus preventing any electron transfer. In this case, the superposition of atomic densities will be exact. Use of $\Delta E_P(A;n)$ in the CEM theory will then introduce an artificial interaction energy due to the intercept at $-EA$. This cannot simply be subtracted out since the extent of any electron transfer at higher electron density (e.g. the breakdown of the electron density superposition approximation) will not be the same as the situation at $n=0$.

To see this in more detail, consider a diatomic molecule AB for example. At a large separation R, the energy required to transfer an electron from B to A is to a good approximation

$$\delta E(A,B) = IP(B) - EA(A) - 1/R \tag{2.23}$$

in obvious notation. These components can be interpreted in the following manner: (*a*) IP(B) is the energy required to remove an electron from the highest occupied atomic orbital (HOAO) of the host which is located at $-IP(B)$; (*b*) $EA(A)$ is the energy gained by filling the lowest unoccupied AO (LUAO) of the atom which is located at $-EA(A)$; (*c*) $-1/R$ is the reorganization energy gained in the transfer of electron density between the two atoms. Equation (2.23) is only correct at large R since at small R the last term would eventually become positive due to both electrostatic and kinetic energy overlap repulsions.

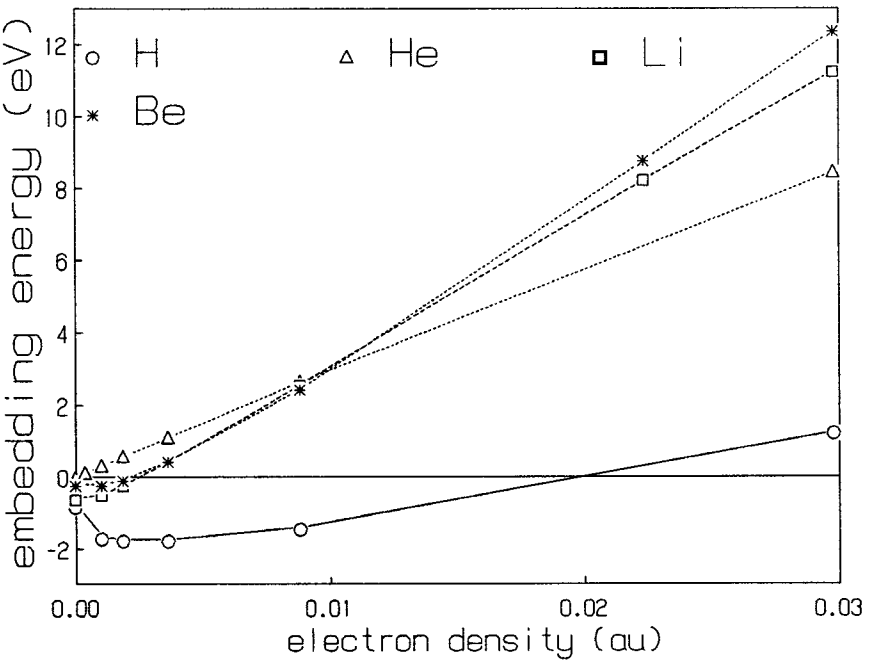

(*a*)

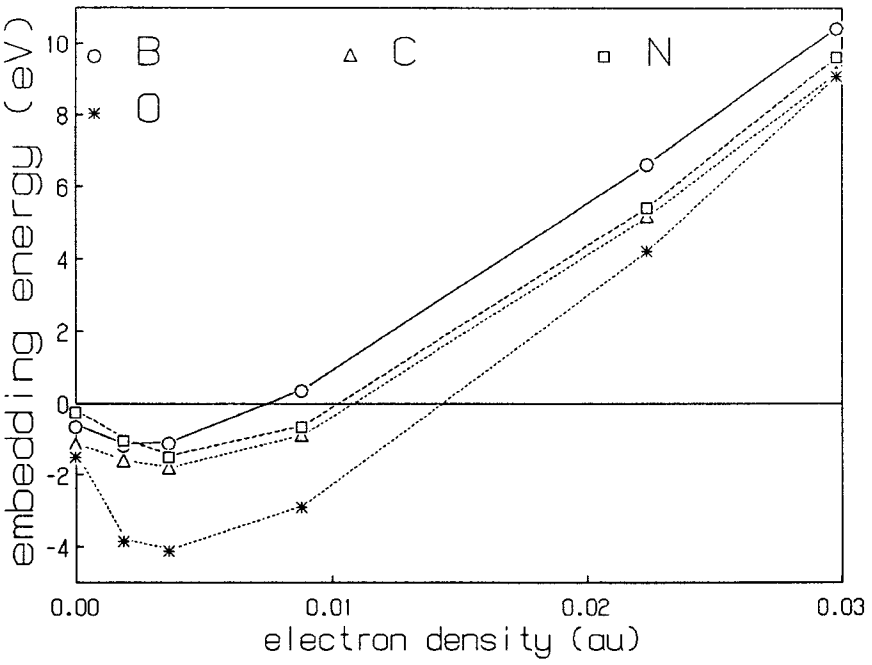

(*b*)

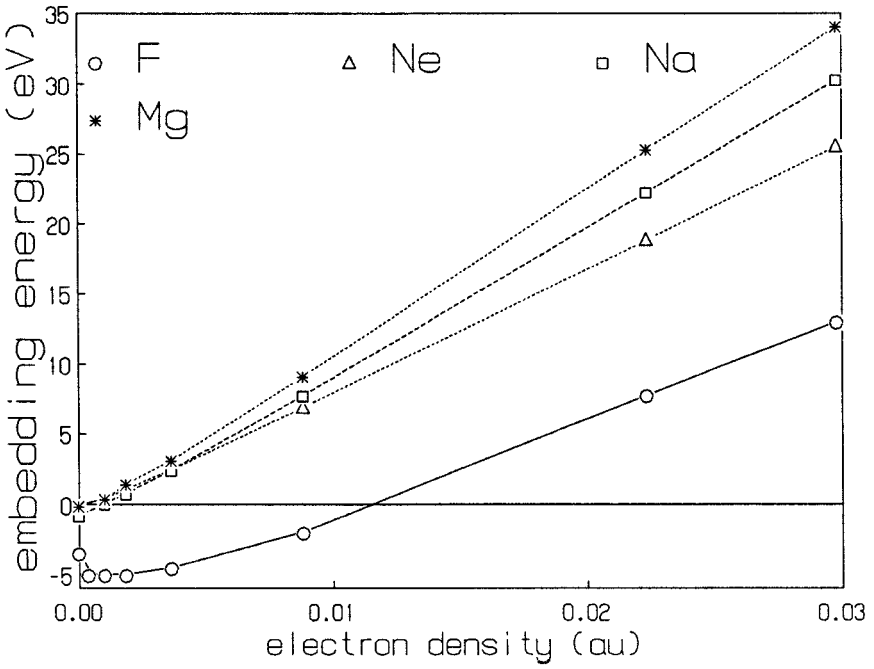

(*c*)

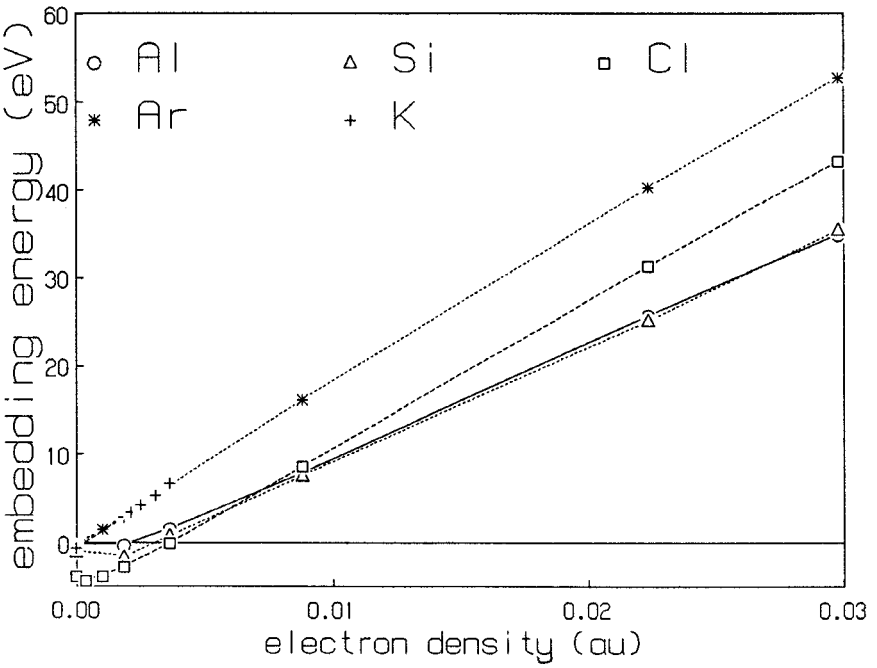

(*d*)

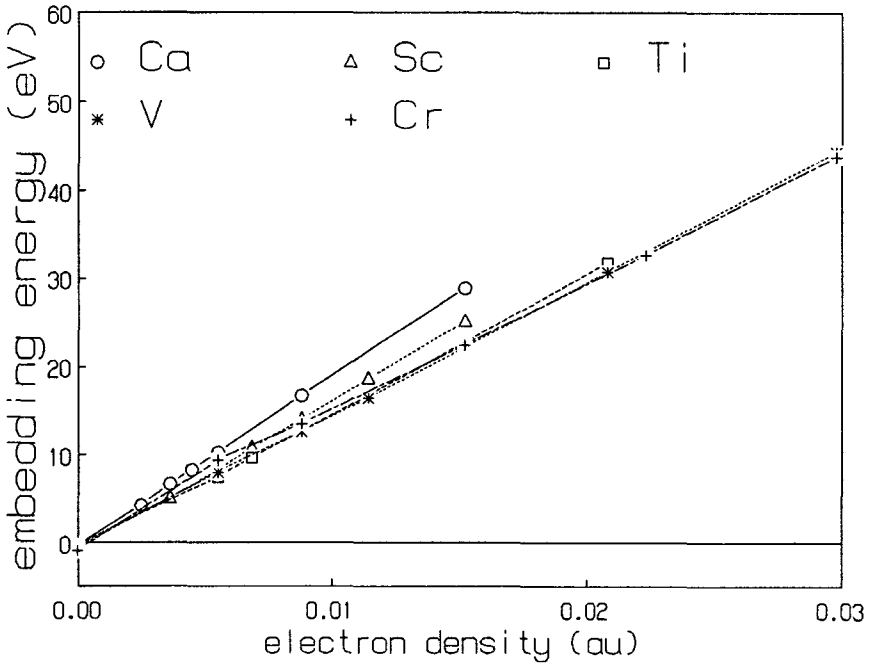

(e)

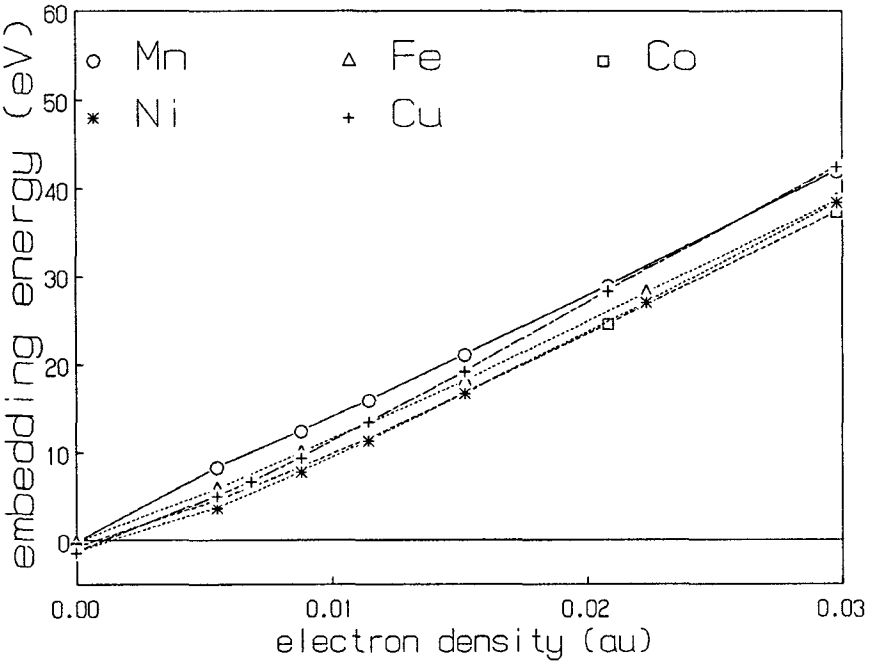

(f)

Figure 1. SCF-LD embedding energies for H through Cu as a function of the jellium electron density (Puska *et al.* 1981, M. J. Puska 1988, private communication).

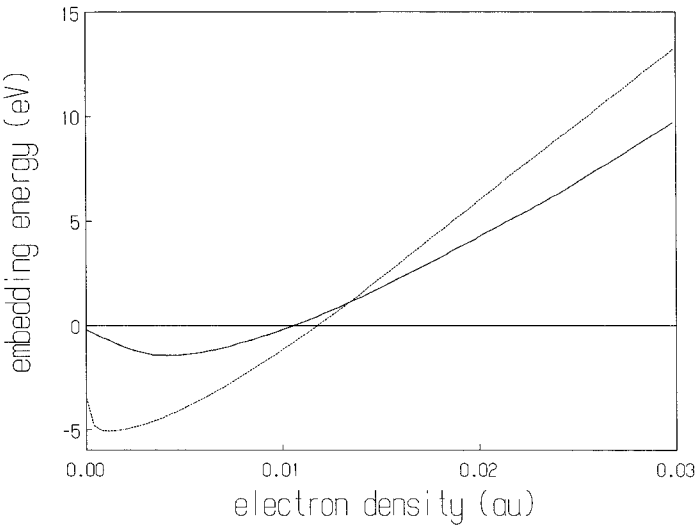

Figure 2. SCF-LD embedding energies for N (——) and F (– – –) as a function of the jellium electron density (Puska *et al.* 1981, M. J. Puska 1988, private communication).

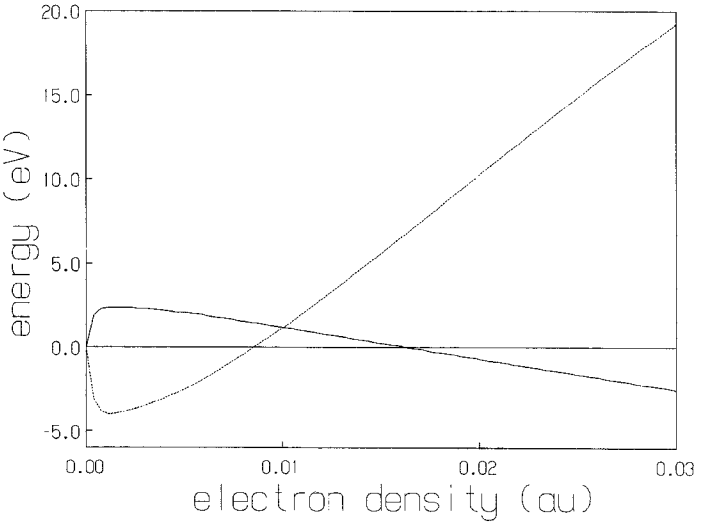

Figure 3. Decomposition of the F atom SCF-LD embedding energy according to equation (2.24) of the text. The EA(F) would appear as a horizontal line at 3·52 eV. (——) work function, (– – –) reorganization energy.

For atom A in jellium, the SCF-LD embedding energy can be written in an analogous form to equation (2.23):

$$\Delta E_{\mathrm{P}}(\mathrm{A};n)=WF(n)-EA(\mathrm{A})+\delta E_{\mathrm{r}}(\mathrm{A};n), \tag{2.24}$$

where $WF(n)$ is the work function of the jellium and $\delta E_{\mathrm{r}}(n)$ is the reorganization energy. The work function depends only upon the jellium electron density and is shown in figure 3. The reorganization energy depends upon each individual atom, and can be calculated by using the known values of $\Delta E_{\mathrm{P}}(\mathrm{A};n)$ The result for F is typical and is also shown in figure 3. The reorganization energy behaves in an analogous manner to $-1/R$: both decrease from zero in the limit of non-interaction, $R\rightarrow\infty$ or $n\rightarrow 0$. In this limit both are simply an extra electrostatic reorganization. At large electron density $\delta E_{\mathrm{r}}(\mathrm{A};n)$ becomes quite positive due to kinetic energy and electrostatic repulsions; this is exactly how the $-1/R$ term would behave in the real system. Thus the main distinction between the jellium and real systems is the difference between the donation of an electron from the Fermi level at $-WF(n)$ in the former case and the donation of an electron from the HOAO at $-IP(\mathrm{B})$ in the latter case.

The above discussion would indicate how to modify the embedding energy, at least for a diatomic system treated within CEM, if the bonding was due to a long-range electron transfer mechanism. However, the real situation involves a mixture of covalent and ionic configurations. Under these circumstances, one must modify $\Delta E_{\mathrm{P}}(\mathrm{A};n)$ using further calculations on the atom embedded into jellium system, with variable work functions. In other words, rather than calculate the actual non-additive densities in each system, we use new embedding functions. We might emphasize that it is a matter of choice whether one considers these changes as a definition of a new funciton or as a correction of ΔG due to non-additive densities, at least for homogeneous systems (i.e. all N atoms of the same chemical identity).

The question then arises as to how to determine these new embedding functions. For non-metallic atoms, we invert the homonuclear diatomic binding curve using equations (2.5) and (2.7 *a*) to yield

$$\Delta E_{\mathrm{C}}(\mathrm{A}_1;n_1)=\{\Delta E(\mathrm{A}_1,\mathrm{A}_2)-V_{\mathrm{c}}(1,2)-\Delta G(\mathrm{A}_1,\mathrm{A}_2)\}/2. \tag{2.25}$$

The subscript C on this function indicates that it describes covalent bonding in contrast to the ionic bonding description evident in ΔE_{P}. By varying the diatomic bond length, it is possible to determine the variation of ΔE_{C} with electron density via equation (2.11 *b*). Results for N and O are shown in figure 4, where a Morse potential was used to generate the binding curves $\Delta E(\mathrm{A}_1,\mathrm{A}_2)$ for N_2 and O_2. It is apparent that $\Delta E_{\mathrm{P}}(N;n)$ and $\Delta E_{\mathrm{C}}(N;n)$ agree rather well while the curves for oxygen disagree very much. This is in accord with the substantially higher electron affinity of oxygen and its affinity to form O^{2-} in jellium but not in O_2.

Further details of these problems can be found in the work of Kress and DePristo (1988). At the present time, there is no solution to the transition from ionic to covalent bonding. Hence application of CEM has been restricted to metals and atomic adsorbates on metals for which the covalent and SCF-LD functions respectively are appropriate. Strongly ionic compounds such as LiF are also difficult to treat since they reflect point-charge-like interactions, an even stronger deviation from the assumption of additive atomic densities. One could always use additive ionic densities but ΔE_{P} are unknown for ions. This is not a particularly severe problem in practice since such simple systems can be treated already using the original Gordon–Kim electron-gas theory with ionic densities (Waldman and Gordon 1979, Muhlhausen and Gordon 1981).

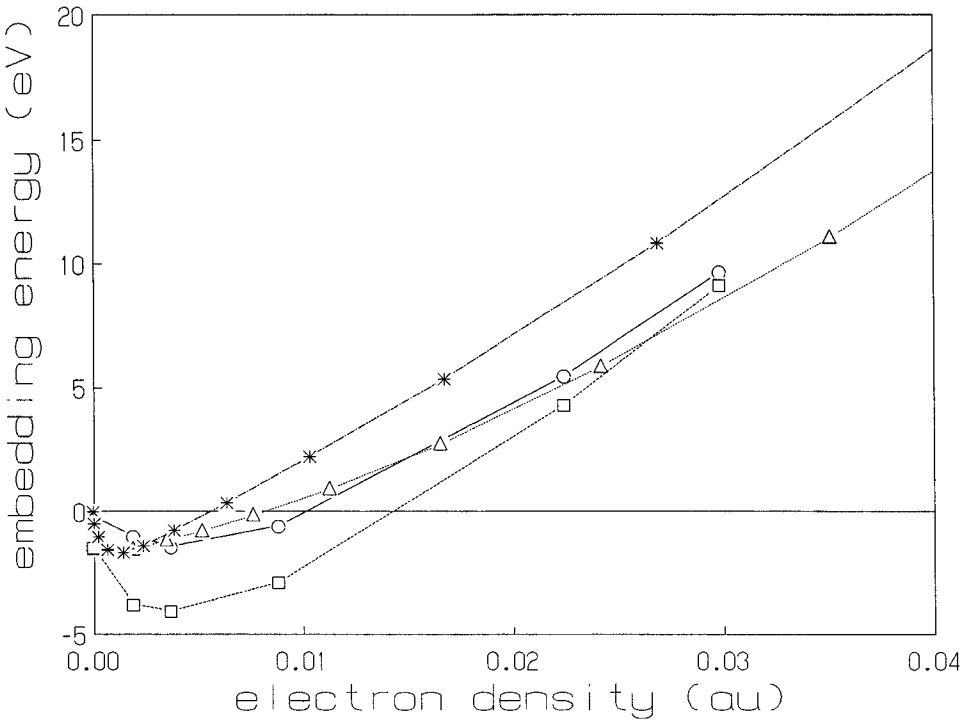

Figure 4. The SCF-LD and CEM covalent embedding functions for N and O. (○) N (SCF-LD), (△) N (covalent), (□) O (SCF-LD) and (*) O (covalent).

For metallic atoms, we also invert the cohesive energy of the bulk system via equation (2.14):

$$\Delta E_C(A_1; n_1) = \Delta E_{coh}(A_1) - \frac{1}{2}\sum_{j\neq 1} V_c(1,j) - \Delta G(\{A_j\})_{WS(1)}. \tag{2.26}$$

By varying both the diatomic and bulk separations around equilibrium, it is possible to determine the variation of ΔE_C with electron density via equation (2.11 *b*). Furthermore, the densities in equations (2.25) and (2.26) will be quite distinct because of the different number of nearest neighbours in a diatomic, 1, *versus* a bulk system, 8–12. The universality of equations (2.25) and (2.26) can be determined by the smoothness of ΔE_C as a function of electron density.

This determination of a new embedding function adds an empirical feature to the CEM method. This will be undesirable if it eliminates the ability to make predictions about the behaviour of new systems. It will be desirable if it determines the energies to high accuracy.

The function ΔE_C is constructed for Ni and Pd using the diatomic Morse potential with parameters determined by fitting to the binding energy, bond length and vibrational frequency. This yields (D_e, α_e, R_e) of (2·092 eV, 1·017 bohr^{-1}, 4·157 bohr) and (1·04 eV, 0·6825 bohr^{-1}, 5·008 bohr) for Ni and Pd respectively (Morse 1986). The points are evaluated at 1·00–1·05R_e in steps of 0·01R_e. The bulk cohesive energy used

the universal binding energy curve (Rose *et al.* 1981) in the form of a Morse curve in the lattice constant,

$$\Delta E_{coh}(a) = D\{\exp[-2\alpha(a-a_0)] - 2\exp[-\alpha(a-a_0)]\}.$$

The values of (D, α, a_0) are (4·44 eV, 0·538464 bohr^{-1}, 6·65 bohr) and (3·89 eV, 0·592743 bohr^{-1}, 7·35 bohr) for Ni and Pd respectively, based upon use of the lattice constant, bulk modulus and cohesive energy (Kittel 1971). The value of α was determined from the bulk modulus of $1{\cdot}86 \times 10^{11}$ J m^{-3} and $1{\cdot}808 \times 10^{11}$ J m^{-3} for Ni and Pd respectively (Kittel 1971). The points are evaluated at $0{\cdot}95$–$1{\cdot}05a_0$ in steps of $0{\cdot}01a_0$. This Morse form should be more accurate than a simple-harmonic expansion.

The functions are shown in figure 5 with the points simply connected by straight line segments for clarity. It is evident that the bulk and diatomic regions join smoothly to provide a universal embedding energy function, at least for covalently bonded systems. We have constructed these functions for a number of metals: Li, Na, Mg, Al, K, Ca, Sc, Ti, V, Cr, Fe, Co, Ni, Cu, Ru, Rh, Pd, Ag, W, Pt and Au. The results for Al and Sc are shown in figure 6. The values for Al are reasonably smooth but those for Sc display a more distinct break between the diatomic and bulk regions. We have seen such non-smooth behaviour for a number of transition metals on the left-hand side of the periodic table.

To understand the problem with Sc in figure 6, remember that the occupations of the atoms are fixed by the HF results in CEM. Thus the embedding functions are determined for a particular atomic configuration. If this configuration changes considerably between the diatomic and the bulk, then the empirical embedding function will not be a universal function. Indeed, the poorly described materials are Sc, Ti, V and Cr which have partially filled d shells that are sphericalized in the present implementation of CEM. This is evidently a gross error in the diatomic since strong directional d bonding can occur. While this error is not intrinsic to the CEM formalism, it is difficult to remove because the occupation of the d shell will change considerably between the diatomic and bulk binding. Such changes likely require some degree of self-consistency to describe.

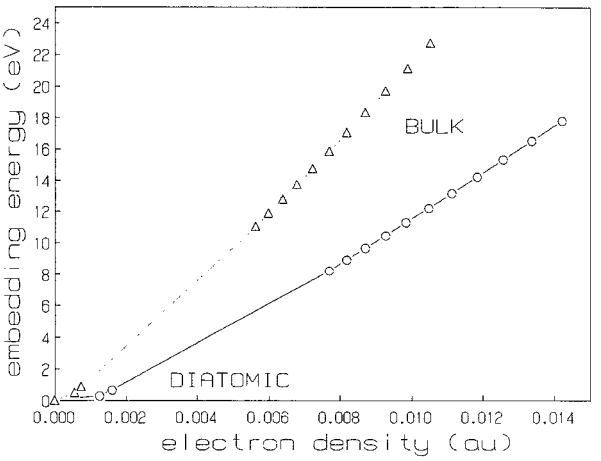

Figure 5. The CEM covalent embedding functions for Ni (○) and Pd (△). The values labelled diatomic are calculated as the bond length varies, with only the $1{\cdot}00R_e$ and $1{\cdot}05R_e$ results shown for clarity. The values labelled bulk are calculated from the monatomic metal as the lattice constant varies from $0{\cdot}95a_0$ until $1{\cdot}05a_0$ in steps of $0{\cdot}01a_0$.

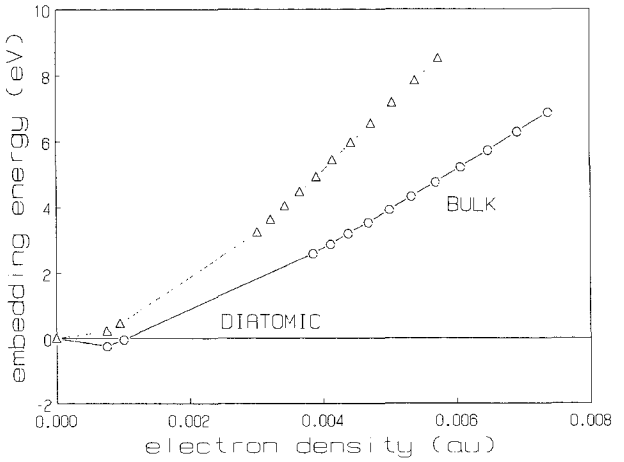

Figure 6. Same as figure 5 except for Al (○) and Sc (△).

It is also worthwhile to note that the covalent functions in figures 5 and 6 are very similar to the SCF-LD functions in figure 1. Thus, for metals, the distinction between use of the two different functions often is just a question of quantitative accuracy, not qualitative differences. This is in distinction to the situation for non-metals such as oxygen in figure 4.

3. Uncorrected and empirical effective-medium-type theories

The computationally time-consuming part of the CEM theory involves evaluation of ΔG. In this section, we review approximations to the CEM theory which lead to a computationally efficient theory (Stave *et al.* 1989, Sanders *et al.* 1990) with acronym MD/MC-CEM. As in the CEM method, the MD/MC-CEM approach is either first principle when based upon the SCF-LD embedding energies or semi-empirical when based upon the covalent embedding energies. Further approximations lead to the well known empirical embedded atom method (Daw and Baskes 1984, Daw 1989), and the very similar 'glue' model (Ercolessi *et al.* 1986, 1987a, 1987b, 1988) and Finnis–Sinclair model (Finnis and Sinclair 1984, Finnis *et al.* 1988).

3.1. *MD/MC-CEM theory*

The central approximation is the incorporation of ΔG into the embedding energies,

$$\sum \Delta F_J(A_i; n_i) = \sum \Delta E_J(A_i; n_i) + \Delta G(\{A_i\}), \tag{3.1}$$

where ΔF_J is a new function of the jellium electron density. This yields the much simpler MD/MC-CEM form for the interaction energy:

$$\Delta E(\{A_i\}) = \sum \Delta F_J(A_i; n_i) + \Delta V_c. \tag{3.2}$$

A formal justification of equation (3.1) requires

$$\Delta G(\{A_i\}) \approx \sum f(A_i; n_i), \tag{3.3}$$

where each f is an arbitrary function of the jellium electron density. This means that a *functional* of the total electron density and its gradient for a particular system is

approximated by a sum of *functions*. Each of these functions pertains to a particular atom in the system and is supposedly universal in the sense of being independent of the particular system under study. If the electron density environment does not change too drastically, this will be an adequate approximation.

For the covalent functions, ΔF_C, we proceed just as in section 2.5, using the homonuclear diatomic binding and the monatomic bulk cohesive energy curves:

$$\Delta F_C(A_1; n_1) = \{\Delta E(A_1, A_2) - V_c(1,2)\}/2, \tag{3.4a}$$

$$\Delta F_C(A_1; n_1) = \Delta E_{coh}(A_1) - \frac{1}{2}\sum_{j\neq 1} V_c(1,j). \tag{3.4b}$$

Hence the new covalent functions are determined in an analogous way to the old functions. Some estimate of the validity of equations (3.4) can be determined by the smoothness of ΔF_C as a function of electron density. However, one should not lose sight of the fact that the approximation in equation (3.2) underlies equation (3.4). Hence the accuracy and validity of the MD/MC-CEM formalism must be lower than those of the CEM formalism.

The function ΔF_C has been constructed for Ni and Pd using the same data as in section 2.5. As shown in figure 7, these functions are rather smooth just as for the functions ΔE_C in figure 5 for the full CEM theory. By contrast, in figure 8, the ΔF_C for Al and Sc are clearly not as smooth as the analogous ΔE_C in figure 6. Thus, the smoothness in the CEM embedding functions for Al, Ni and Pd does not correlate with accuracy in the MD/MC-CEM functions, where Al is now much less smooth. This illustrates an important point. MD/MC-CEM provides a consistency check based upon the fact that lack of smoothness of ΔF_C signals the non-universality of the function. Hence one would have to use caution in the interpretation of any results for Al or Sc which depended upon the embedding function in the electron density region below the bulk values.

Construction of ΔF_J for heteronuclear systems can be more complicated unless the interactions are expected to be similar to the homonuclear case, in which case ΔF_C can be used. If the bonding is expected to be ionic, then equation (3.2) with ΔE_P on the right-hand side may be used. The question of the appropriateness of the embedding function

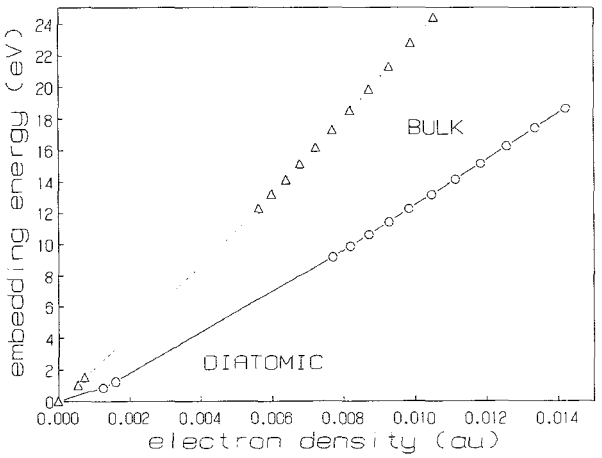

Figure 7. Same as figure 5 except for the MD/MC-CEM embedding function.

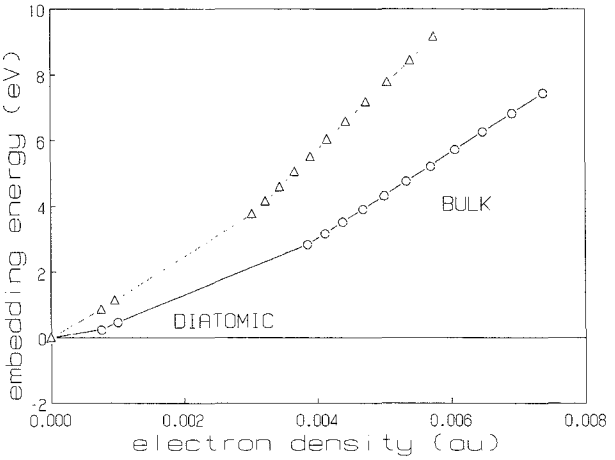

Figure 8. Same as figure 7 except for Al (○) and Sc (△).

ΔF_J for any system is no different than for ΔE_J. Thus, the same caution concerning strong electronegative and electropositive elements must be used as for the full CEM calculations. Indeed, a full CEM calculation can be performed for the system under consideration to determine the adequacy of the type of embedding function chosen. This information, in turn, may be used to determine ΔF_J.

As an example, ΔF_P can be constructed for a single H atom interacting with Pd(111). For Pd the covalent embedding functions, ΔE_C and ΔF_C in figures 5 and 7 can be used. For H the binding interaction will be substantially ionic, implying that $\Delta E_P(H)$ can be used. The CEM interaction energy of the H–Pd(111) system is then

$$\Delta E(H, \{Pd_i\}) = \Delta E_P(H; n_H) + \sum \Delta E_C(Pd_i; n_i) + \Delta V_c(H, \{Pd_i\}) + \Delta G(H, \{Pd_i\}) \quad (3.5)$$

while the energy of the Pd(111) system without the H is

$$\Delta E(\{Pd_i\})^0 = \sum \Delta E_C(Pd_i; n_i^0) + \Delta V_c(\{Pd_i\}) + \Delta G(\{Pd_i\}). \quad (3.6)$$

The superscript 0 indicates that the H atom is absent. The analogous equations within the MD/MC-CEM formalism are

$$\Delta E(H, \{Pd_i\}) = \Delta F_P(H; n_H) + \sum \Delta F_C(Pd_i; n_i) + \Delta V_c(H, \{Pd_i\}), \quad (3.7)$$

$$\Delta E(\{Pd_i\})^0 = \sum \Delta F_C(Pd_i; n_i^0) + \Delta V_c(\{Pd_i\}). \quad (3.8)$$

It is the additional interaction of H with Pd(111), $\Delta E(H, \{Pd_i\}) - \Delta E(\{Pd_i\})^0$, that is required to be reproduced by the two functions, $\Delta E_P(H; n)$ and $\Delta F_P(H; n)$, not the interaction energies, $\Delta E(H, \{Pd_i\})$. The latter include the surface energy of Pd(111) which will not be the same in CEM and MD/MC-CEM forms. In other words, $\Delta E(\{Pd_i\})^0$, differs slightly between equations (3.6) and (3.8) because the function $\Delta F_C(Pd_i; n_i^0)$ is guaranteed to duplicate the binding energy of Pd_2 and Pd(bulk), but not necessarily the surface energy. It would be inconsistent to include this disagreement in the Pd surface energy in the new H-atom embedding function.

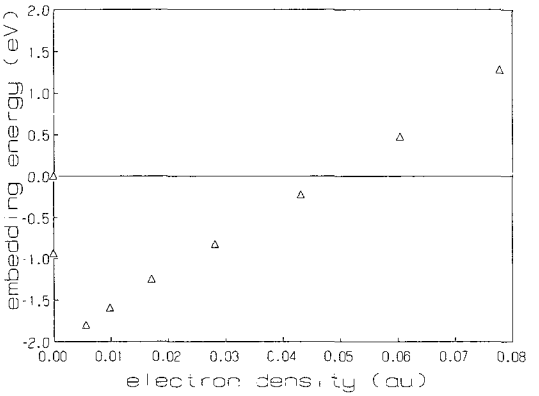

Figure 9. The MD/MC-CEM embedding function for H (△) based upon transformation of the CEM calculations for the H–Pd(111) interaction using the SCF-LD embedding function of Puska *et al.* (1981). See text for more details.

Setting the difference, $\Delta E(\mathrm{H},\{\mathrm{Pd}_i\})-\Delta E(\{\mathrm{Pd}_i\})^0$, equal between the two forms yields

$$\Delta F_{\mathrm{P}}(\mathrm{H};n_{\mathrm{H}})=\Delta E_{\mathrm{P}}(\mathrm{H};n_{\mathrm{H}})+\Delta G(\mathrm{H},\{\mathrm{Pd}_i\})-\Delta G(\{\mathrm{Pd}_i\})$$
$$+\sum[\Delta E_{\mathrm{C}}(\mathrm{Pd}_i;n_i)-\Delta E_{\mathrm{C}}(\mathrm{Pd}_i;n_i^0)-\{\Delta F_{\mathrm{C}}(\mathrm{Pd}_i;n_i)-\Delta F_{\mathrm{C}}(\mathrm{Pd}_i;n_i^0)\}]. \quad (3.9)$$

This expression defines the new embedding function for the H-atom in terms of quantities calculable by the full CEM form. In figure 9, the function $\Delta F_{\mathrm{P}}(\mathrm{H};n)$ is shown. The latter is again quite smooth, implying that it could be used for other faces of Pd and other metals with acceptable accuracy.

3.2. *Embedded atom, 'glue' and Finnis–Sinclair methods*

These methods can be derived by making a number of further, uncontrolled approximations to the MD/MC-CEM method. First, consider equation (2.11 *b*) for the jellium electron density. Assume that the weight function $n(\mathrm{A}_i;\mathbf{r}-\mathbf{r}_i)$ is very peaked around the nucleus, allowing for extraction of $n(\mathrm{A}_j;\mathbf{r}-\mathbf{R}_j)$ at $\mathbf{r}=\mathbf{R}_i$ and ignore the factor of $\frac{1}{2}$:

$$n_i^{(\mathrm{EAM})}=\sum_{i\neq j} n(\mathrm{A}_j;|\mathbf{R}_i-\mathbf{R}_j|). \quad (3.10)$$

This is a so-called pointwise electron-density evaluation. Second, define a new embedding function by subtracting out the high electron-density linearly repulsive region:

$$\Delta F^{(\mathrm{EAM})}(\mathrm{A}_i;n_i)=\Delta F_{\mathrm{C}}(\mathrm{A}_i;n_i)-\gamma_i n_i \quad (3.11\,a)$$

where

$$\gamma_i=\lim_{n_i\to\infty} \mathrm{d}\Delta F_{\mathrm{C}}(\mathrm{A}_i;n_i)/\mathrm{d}n_i. \quad (3.11\,b)$$

Due to the characteristic shape of ΔF_{C}, the new functions, $\Delta F^{(\mathrm{EAM})}$, will be negative for all densities.

Using equations (3.10) and (3.11) in (3.2) and invoking equation (2.7 *a*) yields the EAM expression:

$$\Delta E(\{A_i\}) = \sum \Delta F^{(EAM)}(A_i; n_i) + \frac{1}{2} \sum_j \sum_{i \neq j} V_2(i,j) \tag{3.12a}$$

where the new two-body potentials are given by

$$V_2(i,j) = V_c(i,j) + 2\gamma_i n(A_j; |\mathbf{R}_i - \mathbf{R}_j|). \tag{3.12b}$$

The EAM expression has not been developed along these lines previously. Instead, a completely empirical development has been used. Equation (3.12 *a*) has been simply postulated and the functions determined empirically (Daw and Baskes 1984, Daw 1989). The densities, $n_i(\mathbf{r})$, were not taken from any atomic HF or SCF-LD calculations but were arbitrarily represented as simple exponential functions. The two-body potentials have been represented almost always by a shielded Coulomb form:

$$V_2(i,j) = Z_i(R_{ij}) Z_j(R_{ij}) / R_{ij}, \tag{3.13}$$

where $Z(r)$ is an effective nuclear charge as a function of separation. All functions are determined by fitting to experimental data.

The Finnis–Sinclair method is similar to the EAM but builds in the further restriction that only nearest neighbours contribute to the determination of the jellium electron density. The 'glue' model uses exactly the same form as equation (3.12 *a*) but does not require the two body forms to be totally repulsive or the embedding energy to be totally attractive. In addition, in the 'glue' model, an effective coordination function is used instead of an electron density function.

3.3. *Discussion of semi-empirical and empirical methods*

It is worthwhile to emphasize that in the empirical EAM, 'glue' and Finnis–Sinclair methods, one may use any form for the arbitrary functions and fit any appropriate experimental data (Garrison *et al.* 1988). Indeed, a form similar to the EAM one has been used in treatments of the dissociative chemisorption potential (Lee and DePristo 1986, 1987a, 1987b, Kara and DePristo 1988). In this method, the embedding energies were set equal to ΔE_P, the densities used equation (3.10), and the two-body potentials were represented as Morse forms. Adjustments were made to fit atomic chemisorption energies and dissociative chemisorption probabilities.

The applicability of these empirical methods can only be determined by comparison with more accurate theoretical results or further experimental data. This limits their predictive ability, but such methods are still extremely useful: a good representation of a multi-dimensional PES can be critical.

The empirical and semi-empirical methods all suffer from a lack of generality for both small non-periodic systems and large periodic systems. The MD/MC-CEM method incorporates some degree of generality since the two-body Coulomb forces involve non-empirical densities of the atoms. Furthermore, if the SCF-LD ΔE_P are used, then ΔF_P is not an empirical function at all since it is determined via equation (3.1) with 'J = P'.

In contrast to CEM, MD/MC-CEM obviously cannot be expected to predict the interaction energies of both a diatomic and bulk system with similar accuracy. For example, a very contracted diatomic molecule may yield the same jellium electron density on each atom as occurs in a bulk system at equilibrium; the vast difference in

electron density environment would not be well described without ΔG. Equation (3.1) provides ΔF_j which can only be single-valued for any one system in which there is just one independent distance and one independent jellium electron density.

The pairwise additive Coulomb energies are attractive and the non-additive embedding energies are generally repulsive in MD/MC-CEM. This is exactly the opposite of the EAM form. Furthermore, the renormalization of the repulsions in equation (3.11 *a*) by moving the repulsive embedding energy part into the Coulomb energy is unsatisfactory. This makes the repulsions very complex in form, and in addition, forces the two-body potentials to be redetermined for each new pair of atoms in the EAM, 'glue' and FS methods unless one assumes that the shielded nuclear charge function $Z_i(R)$ is independent of local environment. By contrast, in MD/MC-CEM, the Coulomb integrals are known for any type of pair. Thus only the latter method predicts the behaviour between different types of atoms but the accuracy may be insufficient, of course.

3.4. *Calculation of forces and energies*

Molecular dynamics simulations require fast evaluation of derivatives and Monte Carlo methods require the same for the energy. While the empirical effective-medium-type theories presented in this section are clearly applicable to large systems without making the gross approximation of pairwise additive interactions, it would appear that the MD/MC-CEM method would be at a significant disadvantage. Owing to the complexity of the underlying computations in the MD/MC-CEM form, it is not obvious that this method can be applied to large systems, but MD/MC-CEM can be evaluated just as efficiently as the other methods, and we review the procedure here (Sanders *et al.* 1990).

Define the overlap function

$$S(i,j)=\int n(A_i;\mathbf{r}-\mathbf{R}_i)n(A_j;\mathbf{r}-\mathbf{R}_j)\,d\mathbf{r}. \tag{3.14}$$

Evaluation of forces requires efficient evaluation of $V_c(i,j)$ and $S(i,j)$ and their derivative with respect to nuclear coordinates. These involve simple two-dimensional integrals over the atomic densities. Direct evaluation of these integrals either numerically or analytically, using Gaussian or Slater-type basis functions, is much too slow.

Fitting of some arbitrary function to the $V_c(i,j)$ and $S(i,j)$ would not be a very general solution and, unless one was lucky in providing an accurate fit with a very simple function, the evaluation would still be rather time-consuming. For the desired accuracy, $\pm 10^{-4}$ eV in $V_c(i,j)$ and $\pm 10^{-7}$ bohr^{-3} in $S(i,j)$, such a simple form would be extremely fortuitous. (Note that this accuracy is more than adequate for chemical energies but can easily be increased or decreased depending upon the function that is to be evaluated.)

We illustrate a general numerical approach based upon function representation and smoothing in Chebyshev polynomials (Abramowitz and Stegun 1972). Only spherically symmetric densities are considered. Consider $V_c(i,j;R)$ where $R=|\mathbf{R}_i-\mathbf{R}_j|$. First, the function is approximated by a Chebyshev expansion in $x=R^{-2}$ on the range $[x_<,x_>]$ where $x_<=R_{max}^{-2}$ and $x_>=R_{min}^{-2}$.

$$V_c(i,j;R)=\sum_{k\geq 0} V_T(i,j;k)T_k(t) \tag{3.15 a}$$

where T_k is the Chebyshev polynomial of kth order and

$$t=[x-\tfrac{1}{2}(x_> +x_<)]/[\tfrac{1}{2}(x_> -x_<)]. \tag{3.15b}$$

The expansion coefficients, $V_T(i,j;k)$, are determined by numerical integration using Gauss–Chebyshev quadrature (Abramowitz and Stegun 1972). Less than 25 terms always represented $V_c(i,j;R)$ to better than $\pm 10^{-4}$ eV (and S$(i,j;R)$ to better than $\pm 10^{-7}$). Expanding in R^{-2} eliminates any square-root evaluations and effectively samples the function more in the small R region, where the function varies more rapidly, than in the large R region.† This fitting procedure provides an accurate representation of $V_c(i,j;R)$ along with continuous higher derivatives (well past any order of importance in the dynamics, force-constant evaluation, anharmonicity constant calculation etc.). The expansion is not evaluated directly in the dynamics since it would be too slow and since only smooth first derivatives are required for the forces.

In the second step, the Chebyshev series representation is used to generate a set of function and first derivative values, $\{x_k, f_k, f'_k; k=1,\ldots,M\}$, where f'_k is the derivative with respect to x. These are evaluated at points equally spaced in x with spacing δx in the interval $[x_<, x_>]$. Interpolation of these points is then implemented by passing a piece-wise cubic polynomial through the set. Thus, for $x_\alpha \leqslant x < x_{\alpha+1}$,

$$V_c(i,j;R)=V_c(i,j;R_\alpha)+d\{C_1(i,j;\alpha)+d[C_2(i,j;\alpha)+dC_3(i,j;\alpha)]\} \tag{3.16a}$$

$$\partial V_c(i,j;R)/\partial R=\{C_1(i,j;\alpha)+d[2C_2(i,j;\alpha)+d[3C_3(i,j;\alpha)]\}(-2/R^3) \tag{3.16b}$$

where α is the interval in which x lies, C_k is the coefficient of the kth power term, and

$$d=x-x_\alpha. \tag{3.16c}$$

Since the grid is evenly spaced in x, the interval is found directly as

$$\alpha=1+\text{integer}\,[(x-x_<)/\delta x]. \tag{3.16d}$$

The coefficients are determined by requiring equations (3.16*a*) and (3.16*b*) to be continuous throughout the interval $[x_<, x_>]$. Since higher order derivatives than the first derivative are accessible within the Chebyshev series representation higher order interpolation schemes can be used if needed. Equations (3.16*a–d*) are efficient computationally, since they do not require either square roots or an interval search. (Note that R^3 in equation (3.16*a*) need not be evaluated since it is multiplied by the directional factors $(X/R, Y/R, Z/R)$ in the expression for the total force on any atom.) A similar interpolation scheme has been presented before by Andrea *et al.* (1983).

The final step concerns extrapolation outside the interval $[x_<, x_>]$. For $x<x_<$, (i.e. $R>R_{max}$), it is best to ensure continuity of the functions representing $V_c(i,j)$ and S(i,j) and their derivatives. The extrapolation scheme requires both the function and its derivative to be zero at some cut-off point, $x_0=R_0^{-2}$, and to be continuous with the interpolation scheme at $x=x_<$. To ensure a monotonic approach of the function representing $V_c(i,j)$ and its derivative to zero, we also require that the second derivative with respect to x be non-positive at x_0 and the third derivative be non-positive for all

† It would be more efficient to expand in R^2 but this effectively samples the function more at large R, where the function varies more slowly, leading to much larger storage requirements for the same accuracy.

$x \in [x_0, x_1]$. These conditions specify the coefficients of the cubic polynomial and the possible locations of the cut-off. For $x > x_>$ (i.e. $R < R_{\min}$), extrapolation is done linearly.

This procedure provides a complete solution to the representation of essentially any well behaved (one-dimensional) function and its derivatives. It depends critically upon the properties of Chebyshev series in providing a near minimax fit, and in the ability to generate the function at the relevant Gauss–Chebyshev points for evaluation of the coefficients in the series. This would be available for any analytic function, no matter how complex.

The embedding function, $\Delta F_J(A_i; n_i)$, poses an additional problem since it is known only at a small (< 20) set of points. These data are fitted to Chebyshev series using a weighted linear least-squares procedure. An estimate of the uncertainty of each point in the data set is used to determine its weight. This procedure allows the embedding energy values to adjust slightly to ensure smooth derivatives. The original data set can then be replaced by 30 points distributed along the fitting interval evaluated using this Chebyshev expansion. Once this larger adjusted data set is obtained, a quasi-Hermite spline of the points can be treated as an analytic function and the procedure leading to equations (3.16) followed with $x = n_i$.

To conclude this section, we provide the explicit force on any atom based upon equation (3.2):

$$\mathbf{f}_i = \sum_{j \neq i} \left\{ \frac{1}{2} \left[Z_i^{-1} \left(\frac{\partial \Delta F_J}{\partial n_i} \right) + Z_j^{-1} \left(\frac{\partial \Delta F_J}{\partial n_j} \right) \right] \frac{\partial S(i,j)}{\partial x} + \frac{\partial V_e(i,j)}{\partial x} \right\} \frac{2}{R_{ij}^4} (\mathbf{R}_i - \mathbf{R}_j). \quad (3.17)$$

To evaluate this equation all the n_i must be known. Consequently, it is impossible to evaluate $\mathbf{f}_i$ by one loop over all pairs formed by atom A_i with every other atom. Nonetheless, using the approach described above this complicated, many-body PES can be evaluated at approximately one-half the speed of a simplistic LJ(12, 6) PES. For example, on a CRAY YMP with an efficiently vectorized program, using a constant step size of 10^{-14} s in the Verlet integrator[37] and evolving 256 active Cu atoms embedded in ≈ 2000 fixed Cu atoms for 10^{-12} s took 2·8 s using LJ(12, 6) based forces and 4·7 s for MD/MC-CEM based forces.

For the EAM, 'glue' and Finnis–Sinclair models, the above fitting procedure has not been implemented. Instead, either simple forms or straightforward spline interpolation have been used. This is understandable since the densities are only needed at one point, and even these densities have been just assumed to be simple exponential functions.

4. Applications

The effective-medium-type methods describe the many-body bonding present in metals (via the embedding energies) and are far superior to pairwise additive potentials. At the same time, these methods do not describe the electronic structure of the system explicitly, and thus are limited to description of the energetic variation with geometric arrangement. The MD/MC-CEM, EAM, 'glue', Finnis–Sinclair and EM methods are nearly as efficient to evaluate as simple pair potentials while even the more time consuming CEM method is still much faster than full *ab initio* or first-principles calculations. Thus the new methods are ideal for investigations of systems containing large number of atoms with low symmetry. Many such applications will be reviewed herein.

It is worthwhile to indicate the steps in the set-up and use of each method. For a CEM calculation, one must:

(1) construct atomic electron densities from the Gaussian fit to HF values;
(2) compute electron density overlaps and evaluate the jellium densities, $\{n_i\}$, from equation (2.11 *b*);
(3) evaluate the embedding energies, $\{\Delta E_j(\mathrm{A}_i; n_i)\}$;
(4) compute all pairwise Coulomb energies, $V_c(i,j)$;
(5) calculate ΔG;

In a non-self-consistent calculation step 1 is done only once and steps 2–5 repeated for each new geometry. There are no adjustable parameters or empirical constructs in this prescription once the embedding energies are known. These are constructed either by fitting the CEM results to both the diatomic and bulk data on the respective homonuclear systems or from the SCF-LD calculations. Any further calculation on heterogeneous systems is predictive, as is any other homogeneous calculation (e.g. surface energy).

For an EM calculation, one must:

(1) construct induced atomic electron densities for the atom in jellium;
(2) evaluate $\{n_i\}$ from the electron density tails of the other atoms within the neutrality radius;
(3) evaluate the embedding energies, $\{\Delta E_{\mathrm{EM},i}\}$;
(4) compute atomic sphere corrections;
(5) calculate the difference in one-electron energies between the real and atom-in-jellium systems.

The neutrality radii and $\{\alpha_i\}$ in equation (2.17) must be found once. Parameters for the calculation in step 5 must be determined from experiment. Since the atom-induced electron density determines the jellium electron density n_i in step 2, one should iterate steps 1 and 2 to self-consistency.

For a MD/MC-CEM calculation, one must:

(1) construct atomic electron densities from the Gaussian fit to HF values;
(2) compute electron density overlaps and evaluate the jellium densities, $\{n_i\}$, from equation (2.11 *b*);
(3) evaluate the embedding energies, $\{\Delta F_j(\mathrm{A}_i; n_i)\}$;
(4) compute all pairwise Coulomb energies, $V_c(i,j)$.

As in the CEM method, the only possible empirical feature occurs if the covalent embedding functions are used.

For an EAM, 'glue' and Finnis–Sinclair calculation, one must construct all parts of the energy:

(1) empirical electron density functions;
(2) empirical embedding energies, $\Delta F^{(\mathrm{EAM})}$;
(3) empirical two-body potentials, $V_2(i,j)$.

All of these parts must either be represented as some arbitrary functional form or as numerical data. Given steps 1–3, any calculation proceeds by evaluating the electron density functions at the centres of all other atoms and then using the embedding energy and two-body potentials.

The EAM, 'glue' and Finnis–Sinclair methods, being totally empirical, are much easier for the new user to apply. One is free to choose any functions and use any data to fit these functions. One must be cautious since the separation of two-body potentials and embedding energies is arbitrary because both are empirical. Thus one should re-determine these functions for all types of systems, and not use those for only the homonuclear system.

Numerous applications of the above methods have been published in the literature over the past years and a complete review is not feasible. Here we summarize the applications to date and examine in detail a few which serve to illustrate and compare some of the weaknesses and strengths of the methods. In our opinion, the most important goal is to be able to employ these methods as tools to gain insight into the chemistry or physics of a particular process, not to reproduce experimental data. The few applications are chosen with this criterion in mind.

4.1. *List of applications*

The following is a list of various applications of the methods as determined by a computer search of the literature over the past twenty years. Some of these are simply tests of the methods to describe metallic bonding in situations other than in the bulk. Others are predictions either supporting or contradicting experimental data. We cannot vouch for the completeness of this list, but do feel that it is likely to display all the areas of applications.

4.1.1. *Metallic bonding*

Pure metals and alloys

Cohesive and/or Formation energies (Maarleveld *et al.* 1986, Jacobsen *et al.* 1987, Redfield and Zangwill 1987, Foiles *et al.* 1984)

Interface structures (Foiles *et al.* 1988, Foiles 1989)

Fracture (Daw and Baskes 1987, Baskes *et al.* 1988)

Segregation (Foiles 1985a, 1987a, Lundberg 1987, Underhill 1988, Stegerwald and Wynblatt 1988)

Thermal expansion (Stoltze *et al.* 1987, Foiles and Adams 1989)

Clean surfaces

Structures of alloy surfaces (Chen *et al.* 1986, 1989, Foiles and Daw 1987, Foiles 1987b)

Surface energies and relaxations (Daw and Baskes 1984, Foiles *et al.* 1986, Ting *et al.* 1988, Raeker and DePristo 1989, Sinnott *et al.* 1990)

Surface reconstructions (Manninen and Nørskov 1982, Daw 1986, Foiles 1987c, Daw and Foiles 1987a, Ercolessi *et al.* 1987a, b, Garfalo *et al.* 1987, Dodson 1987a, Dondi *et al.* 1988, Jacobsen and Nørskov 1988, Dodson 1988)

Phonons

Surface (Nelson *et al.* 1988, Ningsheng *et al.* 1988a)

Bulk (Daw and Hatcher 1985, Ningsheng *et al.* 1988b, 1989)

Liquid metals

Bulk properties (Foiles 1985b)

Surface Melting (Carnevali *et al.* 1987, Stoltze *et al.* 1988)

Epitaxy

Metals on Metals (Voter 1988, Foiles 1987d, Dodson 1987b, c, Gilmore *et al.* 1989, Raeker *et al.* 1990, Raeker and DePristo 1990)

4.1.2. *Chemisorption on/in metals*

Atomic chemisorption

Binding energies and structures (Nørskov and Lang 1980, Nørskov, 1982, 1984, Chakraborty *et al.* 1985, Felter *et al.* 1986, Jacobsen and Nørskov 1986, 1987, Lundqvist *et al.* 1987, Daw and Foiles 1987b, Nørskov and Besenbacher 1987, Raeker and DePristo 1990)

Vibrational analysis (Fröyen *et al.* 1986, Holmberg *et al.* 1987)

Desorption (Baskes 1984, Baskes *et al.* 1987, Avouris *et al.* 1988)

Dissociative chemisorption

Dynamics (Lee and DePristo 1986, 1987a, b, Kara and DePristo 1988, Truong *et al.* 1989)

Structures (Foiles *et al.* 1987, Karimi and Vidali 1989a)

Solvation of adsorbates in metals

Hydrogen (Daw *et al.* 1983, Manninen *et al.* 1984, Jena *et al.* 1985, Nordlander *et al.* 1986, Puska *et al.* 1987, McMullen *et al.* 1987, Besenbacher *et al.* 1987, Batalla *et al.* 1987, McMullen *et al.* 1988).

Oxygen (Ronay and Nordlander 1988)

Atom–non-metal surface interactions: adsorption or scattering

Noble Gases (Rao *et al.* 1985, Toigo and Cole 1985, Frigio *et al.* 1986, Karimi and Vidali 1987, Vidali and Karimi 1988, 1989)

Hydrogen (Karimi and Vidali 1989)

He in bulk metals

Nielson (1985), Adams and Wolfer (1988), Wolfer *et al.* (1989)

Ion-implantation in metals

Besenbacher *et al.* (1985), Myers *et al.* (1985a, b, 1986, 1989), Garrison *et al.* (1988)

Semiconductors

Baskes (1987), Baskes *et al.* (1989)

4.2. *Metallic bonding*

4.2.1. *Bulk-metal cohesive energies*

The relative stability of the close-packed f.c.c. and h.c.p. structures *versus* the more open b.c.c. structures may provide insight into the generality of the present effective-medium-type methods. The CEM method has been used to determine the cohesive energies and equilibrium lattice structures for a number of metals in h.c.p., f.c.c. and b.c.c. type structures using ΔE_C. For each type of atom, the embedding energy function is determined from the experimentally observed cohesive energy and structure. It is the relative stability which is of interest, since the absolute stability is correct by definition for the experimentally stable structure.

Table 1. The bulk nearest neighbour distances and cohesive energies as calculated by the CEM method using the embedding function ΔE_C.

Atom	Structure	NND (bohr)	C (bohr)	ΔE_{coh} (eV)
Al	b.c.c.	5·278		−3·370
	f.c.c.	5·399		−3·388
	h.c.p.	5·411	8·837	−3·388
Fe	b.c.c.	4·679		−4·278
	f.c.c.	4·833		−4·298
	h.c.p.	4·884	7·657	−4·286
Ni	b.c.c.	4·587		−4·423
	f.c.c.	4·693		−4·439
	h.c.p.	4·703	7·680	−4·439
Cu	b.c.c.	4·701		−3·470
	f.c.c.	4·813		−3·486
	h.c.p.	4·823	7·877	−3·486
Rh	b.c.c.	4·956		−5·713
	f.c.c.	5·068		−5·744
	h.c.p.	5·077	8·291	−5·744
Pd	b.c.c.	5·076		−3·857
	f.c.c.	5·188		−3·886
	h.c.p.	5·197	8·488	−3·886
Ag	b.c.c.	5·341		−2·925
	f.c.c.	5·457		−2·944
	h.c.p.	5·465	8·924	−2·944
W	b.c.c.	5·164		−8·888
	f.c.c.	5·323		−8·929
	h.c.p.	5·378	8·431	−8·910
Pt	b.c.c.	5·104		−5·790
	f.c.c.	5·222		−5·837
	h.c.p.	5·238	8·553	−5·848
Au	b.c.c.	5·326		−3·770
	f.c.c.	5·435		−3·809
	h.c.p.	5·451	8·902	−3·807

From table 1 it is clear that the CEM method underestimates the stability of b.c.c. materials relative to the close-packed f.c.c. and h.c.p. structures, for example Fe and W are predicted to be slightly more stable as f.c.c. At the same time, CEM also predicts nearly equal stability for b.c.c. and f.c.c./h.c.p. materials, albeit at different bond lengths. Since CEM explicitly includes the effect of electron density inhomogeneity in the ΔG term, it is evidently the sphericalization of the atomic electron density that leads to this underestimation. We expect other effective-medium-type methods to favour the f.c.c./h.c.p. structures even more strongly. Thus one must be cautious in using these theories to predict structures and energetic differences associated with bulk materials.

4.2.2. *Properties of clean surfaces*

With the exception of CEM using ΔE_P and EM, the methods discussed in this review, except EM, describe bulk metallic bonding accurately within a particular

structure by construction. In CEM and MD/MC-CEM, ΔE_C of the metal atom is fitted to reproduce the correct bulk cohesive energy, lattice constant and bulk modulus. In the EAM, 'glue' and Finnis–Sinclair methods, the electron density functions, embedding and two-body terms are fitted to the cohesive energy, lattice constant, bulk modulus, bulk vacancy formation energy and the elastic constants c_{12} and c_{44}. The EM method does not adjust its functions to experimental data and thus is not guaranteed to reproduce the bulk metallic properties.

Many-body interactions are incorporated within each of the methods. In the CEM method, these are included through the embedding function and the correction (ΔG) energies in equation (2.5*a*). In contrast, the EM, MD/MC-CEM, EAM, 'glue' and Finnis–Sinclair models all rely solely on the embedding function.

Since bulk metals are described accurately, prediction of the properties of metal surfaces is a test of the ability of these methods to describe properly the changes in many body metallic bonding with coordination and separation. A successful description of bonding at surfaces will lead to confidence in predictions of other properties where experimental data is either lacking or requires theoretical input for interpretation.

4.2.3. *Surface energies*

Focus on the energy (not free energy) required to cleave a bulk crystal and expose a particular surface geometry. Since this energy is proportional to the amount of surface area, the energy is divided by the total surface area of both newly exposed surfaces and the resulting intensive quantity reported as the surface energy.

The surface energy σ of a semi-infinite surface within CEM is easily calculated as

$$\sigma = \sum_{\alpha=1}^{N} \frac{\Delta E_\alpha - \Delta E_{\text{coh}}}{A}, \tag{4.1}$$

where ΔE_α is the layer cohesive energy as calculated in equation (2.15), ΔE_{coh} is the bulk cohesive energy in equation (2.14) and A is the surface unit-cell area. The sum is over N surface layers leading into the bulk where the bulk cohesive energy is eventually reached after three to four layers. This same expression is used for MD/MC-CEM, EAM, 'glue' and Finnis–Sinclair models with appropriate expressions for ΔE_α.

Within the EM method, the surface energy is calculated analytically (Jacobsen *et al.* 1987) assuming no surface relaxation and only variation of bonding for the surface layer. For N nearest-neighbour atoms in the bulk, we get

$$\sigma = C[1 - \{N/12\}^{\eta/B\eta 2}]^2 + \alpha n_0[\{N/12\}^{\eta/\beta\eta 2} - N/12]/A \tag{4.2.}$$

which includes only the quadratic term in their cohesive energy expression. The η values are the atom exponential electron density parameters; β is the Wigner–Seitz radius ratio; and n_0 is the equilibrium electron density.

Figure 10 shows three low-Miller-index surfaces of a f.c.c. crystal that are examined here. Clearly a substantial change in the many-body bonding character occurs for metal atoms on and near the surface as compared to the bulk. Surface atoms are significantly destabilized by the loss of their neighbours above the plane. This loss is also face-specific since the number and distance to the neighbours differs with face. Thus the surface energy is a function of the exposed surface, with a high surface energy indicating significant instability. This instability may be manifest in structural changes such as relaxation and reconstruction.

We shall examine the surface energies of four different metals, each in a different row on the periodic table. The quality of the results and the trends for these are similar for the other metals in the same row and thus arguments made about these test cases are

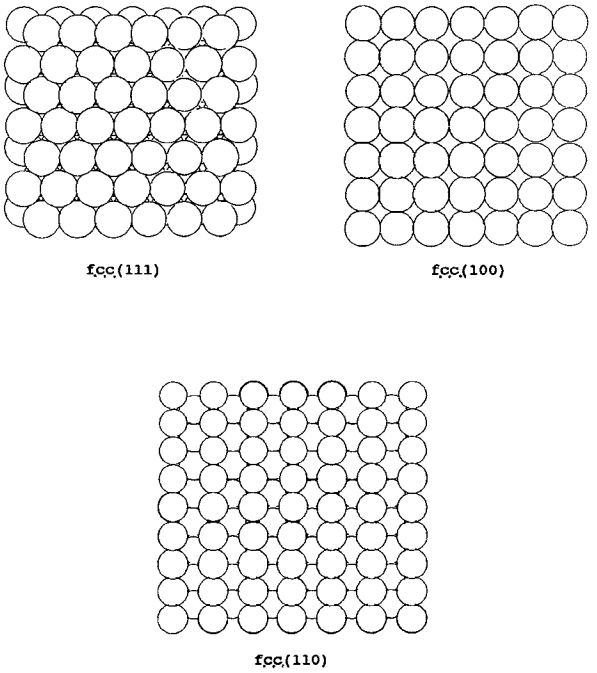

Figure 10. Top view of the f.c.c. (111), (100) and (110) surfaces.

general and easily transferable. The simple metals are represented by Al, the 3d metals by Ni, the 4d by Pd, and the 5d by Pt and Au. Complex metals with substantial d–d bonding are not considered since current effective medium type theories do not describe accurately their structural energy variations.

In table 2 we show the most recent CEM and MD/MC-CEM (Sinnott *et al.* 1990) and EAM surface energies (Foiles *et al.* 1986) for the low-index surfaces of the above metals. The agreement with experimental data is quite good for both types of CEM calculations, especially since the experimental data is an average over a polycrystalline surface. Previous CEM surface energy values (Raeker and DePristo 1989) for some transition metals were about 5% larger than those in table 2. The values here are more accurate since they have used a more accurate Gaussian representation of the atomic HF densities, better numerical evaluation of the correction integral and more accurate interpolation of the embedding function between the lower electron-density diatomic and higher electron-density bulk points. The surface energies confirm that changes in the metallic bonding on surfaces are accurately described by both CEM and MD/MC-CEM. Also note that the surface energy increases with increasing openness of the surface.

Comparing the results from the two different CEM methods, one finds that for the transition metals the surface energies in MD/MC-CEM are always slightly higher. This results from the negative contribution to the surface energy from the correction energy ($\sigma_{\Delta G}$). The approximation of a smooth interpolation of the correction energy between the diatomic and bulk regions of the electron density does not reproduce the effect of the actual calculation of the correction energy.

Table 2. Surface energies ($J\,m^{-2}$) for relaxed geometries of various metals.

Face	Al	Ni	Pd	Pt	Au	Method
(111)	1·120	1·954	1·651	2·002	1·198[a]	CEM
	0·866	2·363	1·906	2·252	1·423[b]	MD/MC-CEM
					1·410[c]	GLUE
	0·247[d]	1·450	1·220	1·440	0·790[e]	EAM
(100)	1·184	2·063	1·756	2·157	1·296[a]	CEM
	0·951	2·474	2·023	2·428	1·543[b]	MD/MC-CEM
					1·635[c]	GLUE
	0·370[d]	1·580	1·370	1·650	0·918[e]	EAM
(110)	1·278	2·230	1·885	2·312	1·384[a]	CEM
	1·047	2·696	2·193	2·615	1·664[b]	MD/MC-CEM
					1·718[c]	GLUE
	0·509[d]	1·730	1·490	1·750	0·980[e]	EAM
Expt.	1·143	2·380	2·000	2·490	1·500[f]	

[a] CEM (Sinnott *et al.* 1990).
[b] MD/MC-CEM (Sinnott *et al.* 1990).
[c] GLUE (Ecolessi *et al.* 1987), includes surface reconstruction.
[d] EAM (Ting *et al.* 1989).
[e] EAM (Foiles *et al.* 1986).
[f] Experimental data on polycrystalline surfaces (Tyson and Miller 1977).

The EAM results consistently yield surface energies that are much too small compared to experiment. In other words, the cohesive energies of the surface atoms are calculated to be much too close to the bulk cohesive energy. The EAM functions do not vary quickly enough with the loss of neighbouring atoms. Previous EAM calculations (Daw and Baskes 1984) also underestimated the surface energies of Ni and Pd. The magnitudes were $1{\cdot}31\,J\,m^{-2}$, $1{\cdot}55\,J\,m^{-2}$ and $1{\cdot}74\,J\,m^{-2}$ for the Ni(111), 100 and (110) surfaces respectively; and $1{\cdot}07\,J\,m^{-2}$, $1{\cdot}27\,J\,m^{-2}$ and $1{\cdot}39\,J\,m^{-2}$ for Pd. This disagreement is difficult to understand since the empirical parameters in the EAM functions were required to reproduce the vacancy formation energy of the metal as well as the bulk cohesive energy and lattice constant. The former should make the empirical functions in EAM describe coordination changes adequately, but the lack of agreement suggests that this is not the case. Alternatively, it may be that the particular separation into two-body and embedding energies is not correct, but is not sensitive to any bulk data which only changes the coordination slightly.

Further EAM calculations of the surface energies of Ni and Cu (Foiles 1985) also resulted in low values. The EAM functions for these calculations were fitted to the above mentioned data and also to the dilute heats of solution of the binary alloys of Cu and Ni. The new EAM functions for Ni resulted in slightly higher surface energies: $1{\cdot}65\,J\,m^{-2}$, $1{\cdot}78\,J\,m^{-2}$ and $1{\cdot}94\,J\,m^{-2}$ for the (111), (100) and (110) surfaces respectively. These values are still significantly smaller than the experimental data. The more recent calculations of the surface energies in table 2 were the result of fitting the EAM functions in the same manner as previously done for Cu and Ni, but with a larger base of heats of solution for the binary alloys of Cu, Ag, Au, Ni, Pd and Pt. Ting *et al.* (1988) also independently fitted EAM functions to experimental bulk data, without alloy data, for the Ni, Pd, Pt and Au systems. They still consistently underestimated the surface energies.

The EM method has also been applied to the calculation of the surface energies for Al surfaces (Jacobsen *et al.* 1987), yielding good results. They obtain values of 0·701, 0·830 and 0·883 J m^{-2} for the (111), (100) and (110) surfaces respectively, compared to the experimental value of 1·143 J m^{-2}. These underestimate the experimental value but are not nearly as small as the EAM results in table 2.

We emphasize that it is now possible to predict the surface energies of metals with good accuracy for spcific faces, using the CEM and MD/MC-CEM methods. The EM method has not been applied to enough metals to be certain, but it appears that it is slightly less accurate than either the CEM or MD/MC-CEM approaches. By contrast, the EAM method substantially underestimates surface energies. This underestimation is not due to the non-uniqueness of the EAM functions, which only causes a slight variation of surface energies. Instead, it appears that the EAM method does not describe properly the variation of metallic bonding with coordination over the coordination range 6–12.

It is interesting to ask why EAM underestimates surface energies while the CEM and EM methods are more accurate, although the EM results for Al are still smaller than experiment. The reason is not certain, but we can correlate this behaviour with the form of the interactions in each method. It has been calculated from SCF-LD calculations (Puska *et al.* 1981, Puska 1988, private communication) that the embedding energy of metals is positive with positive slope at the densities in the bulk. By contast, the EAM embedding energy is parametrized to become increasingly negative with increasing electron density while the pairwise potential is the repulsive term. While any linear term in the embedding energy can be incorporated into the pairwise potential as in equation (3.12 *b*), it may be that fitting directly with attractive embedding and repulsive two-body terms is not accurate. This suggests that the current form of the EAM parametrization is most likely the root of EAM's inability to accurately predict the surface energies.

As further evidence, we note that both the CEM and EM methods provide better surface energies while using embedding functions that are positive and pairwise interactions that are negative. The slight underestimation in the EM method may be due to the $\alpha_i n_i$ term in equation (2.18 *b*) that makes the overall embedding energy negative. This then will result in the same difficulty as the EAM but not to the same extreme. Further evidence comes from the 'glue' model results for Au which are quite good; the 'glue' model uses different embedding, electron density and two-body functions that are much more in accord with the SCF-LD embedding functions.

The above argument is speculative. It is not known why the EAM underestimates the surface energies, and, in most of the literature, it is concluded that EAM values are in good agreement with experimental data. This is true when compared to predictions of simple potentials. However, it is now clear that these surface energies can be calculated much more accurately with other effective-medium-type methods.

4.2.4. *Surface relaxation of Al*

Minimization of the surface energy will lead to relaxation or reconstruction of the surface. The former simply changes the separation between planes of atoms near the surface (typically reported as percentage changes relative to the bulk planar separation) as illustrated in figure 11. Reconstruction changes the in-plane geometries of the surface atoms, and is generally accompanied by relaxation. Both phenomena can be examined

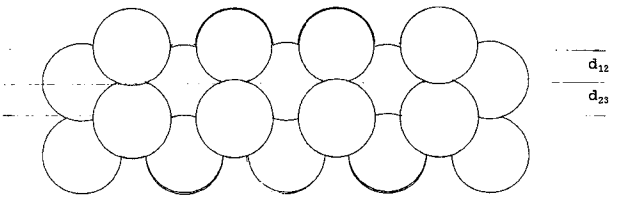

Figure 11. Side view of the f.c.c. (110) surface, d_{12} denotes the distance between layers 1 and 2, d_{23} for layers 2 and 3.

by any of the effective-medium-type methods, which are efficient computationally and, in principle, describe coordination changes properly. In the following sections we shall compare the predictions of the relaxations by the different methods. We have already seen that there is a wide range in the calculated surface energies and that perhaps this may be the case for the magnitudes and even directions of relaxation.

Experimental data indicate that in general the top layer atoms of the surface contract towards the layer below, the contraction increasing for more open surfaces. The f.c.c. (110) surface is observed to exhibit an oscillatory multilayer relaxation with the top layer spacing contracting, the second layer spacing expanding and so on, down to about four layers. First principles SCF-LD calculations by Ho and Bonhen (1985) confirm this feature and indicate that the energy of relaxation is of the order of millielectron volts per surface atom. The CEM, EM, EAM and 'glue' model methods have all been applied to the problem of surface relaxation and reconstruction with varying degrees of success. For the case of CEM, we shall explain the driving forces for relaxation and discuss their relevance to the other two methods.

As a first test, we consider Al, which is a nearly free-electron metal and thus should make the atom-in-jellium approximation very good. In table 3 we show results for the relaxation of Al surfaces. All these methods show that the top layer of all three Al surfaces contract, with the contraction increasing for Al(111)→Al(100)→Al(110), but the predicted magnitudes are clearly different.

In general the CEM, MD/MC-CEM and EM results for the (111) and (100) surfaces are in good agreement with available experimental data. While the experimentally observed (111) top-layer distance expansion is an exception to the general rule of contraction, note that the most recent CEM and EM calculations predict only a very small contraction of around 1% limited to either the top or one subsurface layer. On the other hand, EAM consistently predicts much larger relaxations as far down as four layer spacings deep. The authors make no attempt to explain these predictions.

The results for the (110) surface show that EAM overestimates while CEM, MD/MC-CEM and EM underestimate the degree of multilayer relaxation. For the first set of EAM values (Ting *et al.* 1988) note that the multiple contractions predicted for the (111) and (100) surfaces do not appear for the (110) surface. The reason for this drastic change in behaviour is unknown to us and was not discussed by the authors. In addition, the second set of EAM results (Chen *et al.* 1986) are in almost exact agreement with the first set for Al(110). This agreement is surprising since different two-body potentials (Morse *versus* shielded Coulomb) and embedding functions were used. It would be interesting to know the surface energy as calculated by Chen *et al.* (1986), but this was not reported. The first set of CEM calculations (Raeker and DePristo 1989)

Table 3. Surface relaxation of the (111), (100) and (110) surfaces of Al.

7	Δd_{12}	Δd_{23}	Δd_{34}	Δd_{45}	σ	Method
(111)	−1·0	−0·5			1·120[a]	CEM
	(−3·0	0·5			1·096[b])	CEM
	−0·5	0·0			0·866[c]	MD/MC-CEM
	−1	0			0·701[d]	EM
	−3·26	−1·70	−1·76	−1·83	0·247[e]	EAM
	1·85[f]					expt.
(100)	−0·6	−0·6			1·184[a]	CEM
	(−5·0	3·5	0·5		1·158[b])	CEM
	−2·0	0·5	0·5		0·951[c]	MD/MC-CEM
	−3	0			0·830[d]	EM
	−4·90	−2·24	−2·25	−2·39	0·370[e]	EAM
	−2·2[g]					expt.
(110)	−7·5	−1·5	−0·5		1·278[a]	CEM
	(−9·5	5·5	−1·5	1·0	1·265[b])	CEM
	−7·0	1·5	−1·0	1·0	1·047[c]	MD/MC-CEM
	−7	0			0·883[d]	EM
	−10·47	3·64	−2·93	−1·45	0·508[e]	EAM
	−10·36	3·23	−2·58	−1·58[h]		EAM
	−8·6	5·0	−1·6[i]			expt.

[a] CEM from Sinnott *et al.* (1990).
[b] CEM from Raeker and DePristo (1989).
[c] MD/MC-CEM from Sinnott *et al.* (1990).
[d] EM from Jacobsen and Nørskov (1989).
[e] EAM from Ting *et al.* (1989).
[f] Experimental data from Noonan and Davis (1990).
[g] Experimental data from Bianconi and Bachrach (1974).
[h] EAM from Chen *et al.* (1986).
[i] Experimental data from Anderson *et al.* (1984),

show excellent agreement with experimental data. The loss of second- and third-layer relaxations after the method was computationally improved is discussed in the next subsection on relaxation of Ni surfaces.

The data in table 3 are indicative of the relative accuracies of each method. In the case of CEM the improvement in the Al surface energies after the method was improved to increase numerical precision results in worse agreement for the relaxation of Al(110) but better results for Al(100) and Al(111). EM is very similar to CEM. In the case of EAM the results show sporadic behaviour in relaxation. When coupled with the poor surface energies, one might be inclined to doubt the predictions. The non-uniqueness of the EAM functions do not have much of an effect on the relaxation, at least for Al(110).

4.2.5. *Surface relaxation of Ni*

The relaxation of Ni surfaces has also been studied twice by CEM (Raeker and DePristo 1989, Sinnott *et al.* 1990) and a number of times by EAM (Daw 1984, Foiles 1985, Foiles *et al.* 1986, Chen *et al.* 1986, Ting *et al.* 1988) calculations. In table 4 we summarize a collection of calculated and experimental relaxation data for Ni surfaces. The results vary in detail but all calculations agree that the top layer contracts for the (111), (100) and (110) surfaces.

First consider the CEM results which, in principle, should not differ between two calculations since the embedding energy is determined in the same way for both. In practice, the two sets of CEM calculations differ substantially, just as for Al. The first (Raeker and DePristo 1989) gave a substantial expansion in the second layer distance for the (110) and (100) surfaces while the newer results indicate smaller relaxation of the second- and third-layer distances (Sinnott *et al.* 1990). The reason for this behaviour is the use of the additive atomic electron density *Ansatz*, as discussed in more detail at the end of this subsection. For now, we simply note that MD/MC-CEM yields smaller relaxations, indicating the importance of the correction energy.

We examine this further in figure 12, which displays the changes of the CEM energy components during relaxation. The energies are plotted as a function of the magnitude of the top-layer relaxation of the Ni(100) surface for fixed second and subsequent layers. It is apparent that the embedding and Coulomb energies do not allow any contraction of the top layer distance spacing for this surface, as seen in table 4 for the MD/MC-CEM calculations. (The embedding functions are not the same in CEM and MD/MC-CEM, but they yield the same behaviour here.) It is the correction term, ΔG, which is responsible for the contraction in CEM theory. It is a continually decreasing function

Table 4. Surface relaxations of the (111), (100) and (110) surfaces of Ni.

	Δd_{12}	Δd_{23}	Δd_{34}	Δd_{45}	σ	Method
(111)	−2·5	0·0			1·954[a]	CEM
	0·0	0·0			2·363[b]	MD/MC-CEM
	−2·46				1·310[c]	EAM
	−0·54	0·0			1·450[d]	EAM
	−1·85	−0·04			1·284[e]	EAM
	−1·2[f]					expt.
(100)	−3·2	0·0			2·063[a]	CEM
	(−3·5	2·0			2·320[g])	CEM
	1·0	0·0	0·0		2·474[b]	MD/MC-CEM
	−3·4				1·550[c]	EAM
	−0·23	0·11			1·580[d]	EAM
	−3·04	−0·35	−0·02		1·535[e]	EAM
	−3·2[h]					expt.
(110)	−7·8	0·5			2·230[a]	CEM
	(−9·5	4·0	−1·5	1·0	2·592[g])	CEM
	−1·5	1·0	−0·5	0·5	2·696[b]	MD/MC-CEM
	−8·8				1·740[c]	EAM
	−2·1	0·07			1·730[d]	EAM
	−7·01	1·84	−0·98	0·34	1·733[e]	EAM
	−8·7	3·0	−0·50[i]			expt.

[a] CEM from Sinnott *et al.* (1990).
[b] MD/MC-CEM from Sinnott *et al.* (1990).
[c] EAM from Daw and Baskes (1984).
[d] EAM from Foiles *et al.* (1986).
[e] EAM from Ting *et al.* (1988).
[f] Experimental data from Demuth *et al.* (1975).
[g] CEM from Raeker and DePristo (1989).
[h] Experimental data from Frenken *et al.* (1983).
[i] Experimental data from Adams *et al.* (1985).

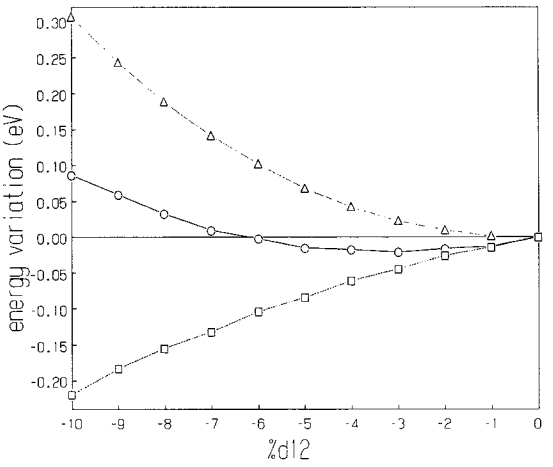

Figure 12. Plots of the changes in the CEM energy components due to relaxation of the Ni(100) top layer distance (○) surface energy (eV), (△) sum of embedding and Coulomb energies ($\Delta E_J + \Delta V$), (□) correction energy (ΔG).

of the contraction which, when combined with the above embedding and Coulomb energies, has a minimum around a 3% contraction as in table 4 for Ni(100). We conclude that relaxation occurs in order to smooth the electron density (which lowers the correction energy) near the surface. This type of smoothing argument has previously been discussed by Zangwill (1988) using jellium ideas.

The first EAM calculations (Daw and Baskes 1984) of Ni relaxation provided top-layer contractions in reasonable agreement with experiment. It would seem at first glance that the already discussed underestimation of the surface energies is unimportant for surface relaxation. Additional calculations (Foiles *et al.* 1986) using a different set of EAM functions that changed the surface energies only slightly, however, resulted in very different relaxations that are in disagreement with experiment. More recent EAM calculations (Ting *et al.* 1988) predicted relaxations that are slightly smaller than experiment and which show an expansion of the second layer distance for the (110) surface.

Thus the unusual situation arises in which each independent EAM calculation results in significant differences in relaxation with only very small differences in the surface energies. In other words, the accuracy of the surface relaxation is not dependent on the accuracy of the surface energy, which is certainly counter-intuitive. However, when one realizes that the variation of surface energy with relaxation is a very small fraction of the surface energy, it is apparent that the calculated relaxations must be extremely sensitive to the fitting of the EAM functions to experimental bulk data. Changing the functions to reproduce a particular bulk property has serious consequences for another, at least for relaxation, even though the non-uniqueness of the EAM functions does not change surface energies substantially.

The CEM method does not predict the correct relaxation in the second and third layer distance spacings. This problem is a consequence of the use of atomic electron densities, as we shall now clarify. The previous CEM calculations of Raeker and DePristo (1989) used even-tempered Gaussian basis functions that were fitted to the

HF atomic electron density, but the tails of the Gaussian densities were larger and of longer range than the HF densities. This electron density produced the large relaxations observed in tables 3 and 4. We have recently provided a much better fit of the HF electron density, and use of this new electron density produced smaller relaxations (Sinnott *et al.* 1990). This is a significant correlation because the electron density in a bulk solid is more delocalized than the superposition of free-atom densities. The poorly fitted Gaussians (unintentionally) mimicked this delocalization, leading to larger overlaps and thus sensitivities of the second-layer atoms to contraction of the first layer. From this argument we see that the approximation of atomic electron-density superposition is likely to be the cause of the underestimation of the multilayer relaxations.

In summary, all three of the methods at least predict that the top-layer distance of a surface is contracted. The large variation of the relaxations in the second and deeper layers indicates weakness in each method that must be overcome if they are to be used as quantitative tools in studying such phenomena on surfaces. We suggest that accurate first-principles calculations on a number of surface systems be used to determine the surface energies and relaxations, especially for the second- and third-layer spacings. These data would be of great utility in determining what is required of effective-medium-type methods to achieve the proper surface energies and relaxations.

4.2.6. *Surface reconstruction of f.c.c. (110) surfaces*

Reconstructions of metal surfaces have been well documented in the literature and in some cases the mode of reconstruction has been established. An important question is whether the effective-medium-type methods predict both the occurrence of reconstruction and the correct reconstructed structure. Although the small surface energy changes upon relaxation are not described consistently by any of the methods, the extension to reconstruction is a natural step since it may lead to large changes in the surface energy.

One type of reconstruction that has been studied by a number of the effective medium type methods is the f.c.c. (110) (1 × 2) reconstruction. LEED measurements (Moritz and Wolf 1985, Chan and Van Hove 1986) have been done on Au(110) and

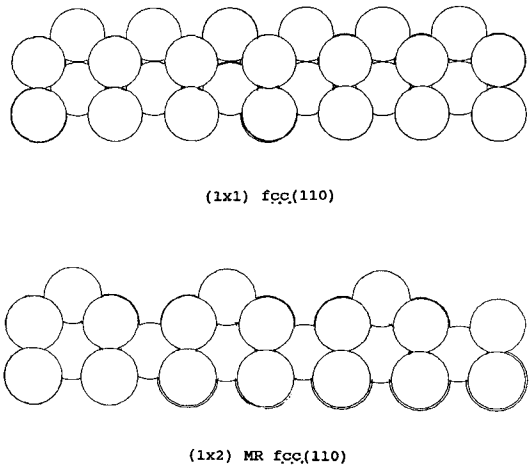

Figure 13. Side view of the (1 × 1) f.c.c. (110) surface and the (1 × 2) MR surface.

Pt(110) revealing a (1 × 2) pattern. The missing row (MR) structure in figure 13, where every other (011) row is missing, has consistently been the model of choice. The driving force for the (1 × 2) MR structure is believed to be faceting to expose the more stable (111) surface plane in the long troughs of the surface.

Generally, all the methods have been employed to determine if the (1 × 2) MR surface has a lower surface energy than the ideal (1 × 1) or other (1 × 2) structures. Each has confirmed that the (1 × 2) MR model has a lower, or at least the same, surface energy as the (1 × 1) structure and that relaxations are present as well.

The 'glue' model has been applied only to the reconstruction of Au surfaces (Ercolessi *et al.* 1987, Garofalo *et al.* 1987). The surface energies are calculated to be (Ercolessi *et al.* 1987) 1·410, 1·635 and 1·718 J m^{-2} for the reconstructed (111), (100) and (110) surfaces respectively, compared to an experimental value of 1·500 J m^{-2} for a polycrystaline sample. Agreement with experiment is quite good, demonstrating that the 'glue' model predicts correctly the instability of these reconstructed surfaces. In particular, note that the (111) surface has a much lower surface energy than the (110) surface.

Molecular-dynamics simulations were used to search for an energetically favourable structure of a particular (1 × *n*) missing row configuration. Here (*n*) stands for (*n* − 1) empty rows between fixed rows of atoms in the top layer and (*n* − 2) empty rows in the second layer and so on for $n \geqslant 3$. The (1 × 2) MR structure was the most stable of the configurations and displayed contractions of 27·5%, 4·7% and 2·2% in the first through third layer spacings respectively. The energy of reconstruction is calculated to be 0·688 J m^{-2} relative to the bulk terminated (110) surface, with relaxation contributing the most to the greater stability of the (1 × 2) MR surface.

For the unreconstructed surface, they calculated a contraction of 33·9% for the first reconstructions followed by expansions of 6·9% and 1·3% in the second and third layers, respectively. The energy of simply relaxing the (1 × 1) surface was calculated to be 0·446 J m^{-2}. This yields an energy of reconstruction relative to the relaxed (1 × 1) surface of 0·242 J m^{-2}.

The calculated (1 × 2) layer spacings differ greatly from the experimental results of contraction by 18–20%, expansion by 2–4% and contraction by 2% in the first three layers, respectively (Moritz and Wolf 1985, Copel and Gustafsson 1986). It is very surprising that the (1 × 1) structure is predicted to contract more than the open (1 × 2) structure.

The EAM was also used to examine the Au(110) (1 × 2) MR surface (Foiles 1987), confirming that the MR model is indeed the most stable structure. The EAM functions were those used in calculation of the surface energies in table 2. The energy of reconstruction to the most stable (1 × 2) MR structure was calculated to be 0·368 J m^{-2} relative to the relaxed (110) surface above, a slightly larger value than that of the 'glue' model. This work showed a contraction of the top three layer spacings of 14·6%, 4·8% and 0·7% with small pairings and buckling in the second- and third-layer atoms respectively.

More recent EAM Monte Carlo calculations (Daw and Foiles 1987) on the order–disorder transition of the (1 × 2) MR Au(110) surface showed a transition temperature of 570 K compared to an experimental LEED-determined transition at 650 K. These calculations followed the transition of an original (1 × 2) MR structure to a disordered one with the same coverage of surface atoms.

Just as in the 'glue' model, the EAM calculations determined that relaxation was not required for the increased stability of the (1 × 2) over (1 × 1) surfaces. This is difficult

to understand. We would expect the loss of neighbours by the surface atoms during reconstruction to cause destabilization and thus increase the surface energy. To lower the surface energy, the surface would contract just as was seen for the clean unreconstructed surfaces in the previous discussions.

It is seen experimentally that the clean f.c.c. (110) surfaces of only Ir, Pt and Au reconstruct. The (110) surfaces of Ni, Cu, Rh, Pd, and Ag can be induced to a (1×2) reconstruction by adsorption of alkali metals, in particular by K, with the proposed structure being very similar to the MR one. The EM method has been applied to the K on Cu(110) system (Jacobsen and Nørskov 1988). The K atoms bind in the open centre sites vacated by Cu atoms from the (1×1) structure. Being so large, they can stabilize the Cu atoms in the remaining rows. At higher coverage, repulsions among the K atoms prevent binding in these open sites. Thus the EM results indicate that the large size of the K atom at low coverage is the main reason for the induced MR reconstruction, with higher K coverage inhibiting this structure. This is a good example of the usefulness of the EM method in understanding the physics of a process and not just in reproducing experimental numbers.

4.2.7. *Surface segregation*

In this section we consider the properties of binary metal alloys, a more chemical problem. Binary alloys often have properties, such as catalytic activity and strength, that differ from those of the separate components. An understanding of the processes that limit alloying is very important. The segregation of one of the components to the surface, causing an enrichment of that atom type relative to the bulk concentration, is one such process. It is well established (Ossi 1988 and references therein) that surface segregation occurs for many mixtures.

A number of simple statistical theories (Mediema 1978, Chelikowsky 1984, Mukherjee and Moran-Lopez 1987) have been introduced based upon the premise that the relative surface energies are important driving factors for surface segregation. The metal with the lower surface energy is enriched at the surface. A limitation of these theories however, is the inability to predict quantitatively the degree of segregation. An alternative to statistical theories is an atom-based approach which correctly describes the relative surface energies of the components in binary alloys and is efficient enough computationally to treat many atoms in a low-symmetry environment. All of the effective-medium-type theories, with the (possible) exception of the more computationally demanding CEM method, are applicable directly.

For the particular case of the EAM method, the fact that the EAM functions are fitted to the dilute heats of solutions of binary alloys and bulk vacancy energies would lead one to expect a proper description of the segregation process. Although the EAM has been applied to many alloy systems, as examples we will examine the Cu–Ni(111) (Foiles 1985a) and, briefly, the Ni–Pt (Lundberg 1987) systems.

From table 2, it can be seen that in EAM the Cu(111) surface has a smaller surface energy than Ni(111). The first calculated quantity was the segregation energy of one impurity atom (Cu) to the Ni(111) surface (Foiles 1985a). This was determined as the total energy of the slab with one impurity atom in the surface layer minus the total energy of the slab with one impurity atom in the bulk. This yielded values of $-0{\cdot}426$ and $-0{\cdot}304$ eV for Cu in Ni(100) and Ni(111) respectively. The former should be compared to an experimental estimate of $-0{\cdot}43$ eV for Cu in Ni(100) (Egelhoff 1983, 1984). This agreement is probably fortuitously good since the EAM functions were fitted to the dilute heats of solutions and thus the Cu impurity in bulk Ni is exact. The

other part of the calculation, involving the surface-energy values, would not be expected to be this accurate based on table 2. Irrespective of the numerical accuracy, the EAM results indicated that in Cu_xNi_{1-x} alloys Cu would segregate to the surface and this segregation would be face-sensitive.

Monte Carlo calculations of the composition using the EAM (Foiles 1985a) yielded the results shown in figure 14, which were in good agreement with experimental data. Interestingly, the calculations also suggested that the second layer is in turn enriched in Ni atoms. No explanation was offered for this phenomenon. It could result from kinetic limitations or too few Monte Carlo moves, or could be a real equilibrium effect. It is certainly worth further study.

In calculations performed for this review, Sinnott has applied the CEM method to a single Cu atom in Ni(100), not in a dynamical simulation, but just to calculate the surface segregation energy. The prediction of −0·3 eV is in good agreement with Egelhoff's value, especially when one remembers that the CEM embedding functions for Cu and Ni are determined solely by the homogeneous bulk and diatomic systems. A similar calculation for an entire Cu layer in Ni(100) predicts −0·286 eV. Segregation of a Cu layer is slightly less stable than a single atom.

The MD/MC-CEM method has been applied to segregation in alloys of metal clusters (Stave and DePristo 1990). For mixtures of Cu and Ni atoms, they find that Cu segregates very strongly to the outside of the clusters. For large clusters, the Cu atoms completely surround the Ni atoms, an effect which is directly analogous to surface segregation. For small clusters, Cu does not segregate to outer surfaces but instead Cu and Ni atoms segregate to different regions of the cluster. Insolubility rather than segregation appears to occur. Again these are predictions since the MD/MC-CEM embedding functions are determined by the homogeneous system. Trimetallic and more complex mixtures would be no more difficult to treat than a single component cluster (Kress *et al.* 1989).

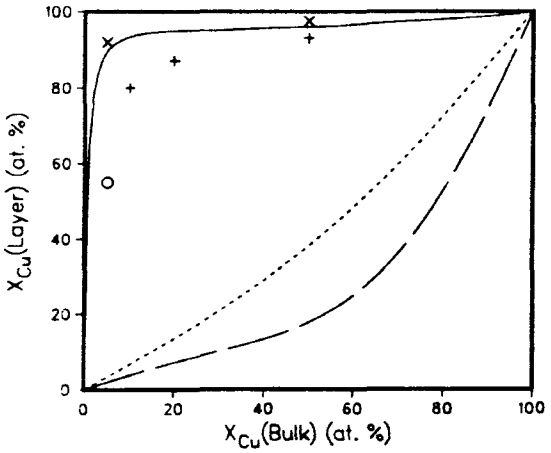

Figure 14. Calculated Cu layer concentrations as a function of bulk composition at $T=800$ K for the (111) face of Ni–Cu alloys. The solid curve is the top layer, the long-dashed curve is the second layer, and the short-dashed curve is the third layer. The points are the experimental values for the top layer (○), Ng *et al.* (1979), (×), Webber *et al.* (1981), (+), Brongersma *et al.* (1978). Reproduced with permission (Foiles 1985a).

Experimentally, it has been observed that for Ni–Pt alloys the (111) and (110) surface exhibit different segregation (Gauthier *et al.* 1987). The (111) surface was enriched in Pt while the (110) surface was enriched in Ni. Lundberg (1987) has confirmed this reversal but does not elaborate on why this occurs. The finding is very interesting since the surface energy of a polycrystalline surface of Ni is slightly less than that of Pt, namely 2·38 and 2·49 J m^{-2} respectively, leading one to expect that Ni would be enriched in both surfaces.

The different segregation observed may indicate that the relative face-dependent surface energies are reversed, since the averages are very close. This is indeed found by EAM calculations (Foiles *et al.* 1986) in table 2, where the Ni(110) surface energy is slightly smaller than the Pt(110) surface but the Ni(111) surface energy is slightly larger than the Pt(111) surface. Whether a very small difference in surface energies is sufficient to explain the data is not apparent. One should also consider the different size of the Ni and Pt atoms. And, when the surface energy is sufficiently close, the segregation may be sensitive to temperature due to entropic effects. Since all of these are included using Monte Carlo simulations and the effective-medium-type methods, it should be possible to determine the surface-face dependence of segregation for all the methods. This would provide a critical test of the various approaches.

4.2.8. *Atomic chemisorption on metal surfaces*

There is an extensive body of experimental data on the energetics and structures of various adsorbates on metal surfaces. Generally, atoms chemisorb in electron-rich sites on a surface (i.e. the fourfold-centre site of f.c.c. (100)), effectively maximizing the coordination with substrate metal atoms. Molecules such as CO may bind to lower coordination sites due to the strong directional nature of the molecular orbitals.

The EM theory has been applied to the binding of H atoms on the most close-packed surfaces of transition metals (Nørskov 1984) with the results shown in figure 15.

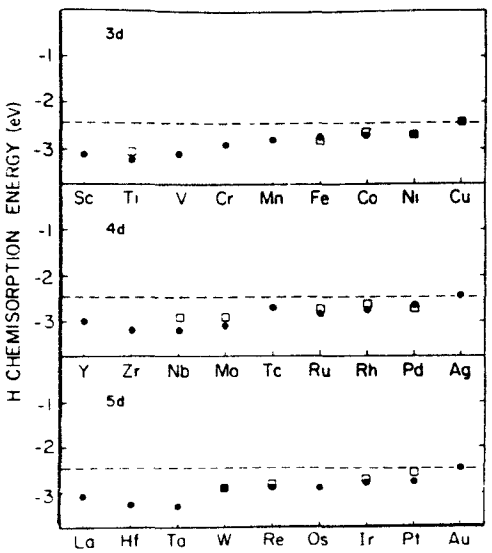

Figure 15. Comparison between calculated (●) and experimental (□) chemisorption energies for hydrogen on the most closed packed surface of each of the transition metals. Reproduced with permission (Nørskov 1984).

The predicted binding energies are in very good agreement with experimental data, especially regarding the correct trends in the relative bonding strengths on different metals.

Because of the computational ease of these methods, they can be used to determine structural parameters, such as the binding height and sites, which aids experimental work on similar systems. One example involves the chemisorption of H on Ni surfaces. Correct predictions of the geometry (Nørskov 1982) of H on Ni(111) compared to experimental data led to confidence in the predictions of H on the Ni(100) and (110) surfaces. The geometry on the latter surface was not in a symmetric site, but rather in a pseudo-threefold binding location.

The bonding of adsorbates on metal surfaces can also have an effect on the structure of the surface. We have already discussed the effect that K atoms have on the Cu(110) surface. What effect does a smaller, more tightly bound, species have on the Cu(110) surface? A recent EM calculation (Jacobsen and Nørskov 1987) showed that a low coverage of chemisorbed H induces an expansion of the top-layer distance of the Cu(110) by about 4%. The induced expansion increased with coverage in agreement with recent LEED experiments (Baddorf *et al.* 1988). In addition, for subsurface H the induced expansion was even larger. This expansion stabilized the subsurface occupation but not enough to favour subsurface over surface chemisorption.

Within the EM method, the physical basis for induced expansion is very simple, and is the inverse of the mechanism for contractions of a clear surface. The adsorption of H atoms to a surface with optimal geometry increases the electron density on the surface atoms above the previous optimal value. Thus the surface metal atoms expand away from the subsurface metal atoms to lower the electron-density environment.

CEM calculations (Raeker and DePristo 1990) have been done for H and N atoms on Fe and W surfaces. The calculated binding energies and heights were in very good agreement with available experimental data. Adsorbate-induced expansion was also found in these systems, with the N atoms inducing over twice the expansion compared to H.

The calculations revealed another mechanism driving the expansion, namely coupling between the adsorbate and second-layer metal atoms. If the adsorbate was close to a second-layer atom, the interaction between them could be greater than the metal–metal interaction. This caused the adsorbate to be attracted to the second-layer atom which in turn pushed the top-layer atoms away slightly. This explained the effect of coverage and relative binding strengths. If more adsorbates interacted with second-layer atoms, the top layer was pushed away even more. In addition, the greater the adsorbate–surface interaction, the closer the adsorbate could get and induce greater expansions.

Both the EM and CEM calculations suggested basically the same mechanism behind the adsorbate induced expansions. Calculations such as these illustrated a real strength of the effective-medium-type methods. Not only could experimental data be reproduced but also one learned about the driving forces behind structural changes on surfaces.

4.2.8. *Dynamical phenomena*

4.2.8.1. *Surface melting*

Recent observations have determined that the top layers of Al(110) and Pb(110) begin to disorder about 150 K below the bulk melting temperatures, T_m (Frenken and

van der Veen 1985, von Blackenhagen *et al.* 1987, Pluis *et al.* 1987). The Al(111) surface was observed to melt only about 50 K below T_m. The thickness of the melted region gradually increased up to just below T_m, suggesting that the surface is the nucleation centre for the melting process.

Theoretical simulations of this process have used large-scale molecular-dynamics simulations. Most attempts have used simplistic Lennard-Jones-type pairwise additive interaction potentials, which do not properly describe metallic binding. Of the effective-medium-type methods, to the best of our knowledge, only the EM method (Stoltze *et al.* 1988) and 'glue' model (Carnevali *et al.* 1987) have been used to examine surface melting.

The EM calculations on the melting of Al surfaces showed that the Al(110) face melts at about 200 K below the calculated bulk melting temperature. The melted surface region propagates gradually into the bulk solid as the temperature approaches T_m. The Al(111) surface on the other hand showed a much weaker surface melting effect below T_m. This demonstrated that the relative stability of the various surface faces played an important role in the initiation of bulk melting. As the surface stability increases (i.e. lower surface energy), the temperature required for surface melting also increases.

Application of the 'glue' model to the surface melting of Au(111) discovered a very interesting feature. When a non-reconstructed Au(111) surface was used, the top surface layers melted about 100 K below the calculated T_m. However, the more stable reconstructed surface, which is a slightly more close-packed hexagonal structure, resisted melting and retained its 'crystalline' form as high as 150 K above the calculated bulk melting temperature. The important point is that the unreconstructed surface melted at 250 K below the reconstructed surface, since the calculated temperatures may not agree with the experimental data owing to inaccuracies in the model. These calculations, on a microscopic scale, illustrated the role that surface reconstruction can have on melting.

4.2.8.2. *High-energy ion sputtering*

A major accomplishment of all effective-medium-type methods is the ability to describe efficiently and properly many-body interactions. This has been tested for the medium-energy range (electronvolts) by the calculations of surface energies. Here we examine interaction energies on the order of kiloelectronvolts using high-energy scattering.

A classical trajectory study of the ejection of Rh atoms from kiloelectronvolt Ar-ion bombardment of the Rh(111) surface (Garrison *et al.* 1988) has recently been done. The EAM functions used in this study were fitted to bulk data, as in most previous work, but in addition the high-energy region of the Rh–Rh potential was used (Torrens 1972). They found that the EAM was able to reproduce experimental kinetic energy distributions of ejected Rh atoms better than the additive pairwise potentials, as shown in figure 16. Many-body interactions, which were important in the ejection process, were well described by the EAM method.

The increased stability of Rh(111) in the EAM *versus* pair potential descriptions was proposed as the reason for the shift in the peak of the kinetic energy distribution to higher energies. Since the EAM consistently overestimates the stability of the surface, shifting of the peak is probably enhanced too much.

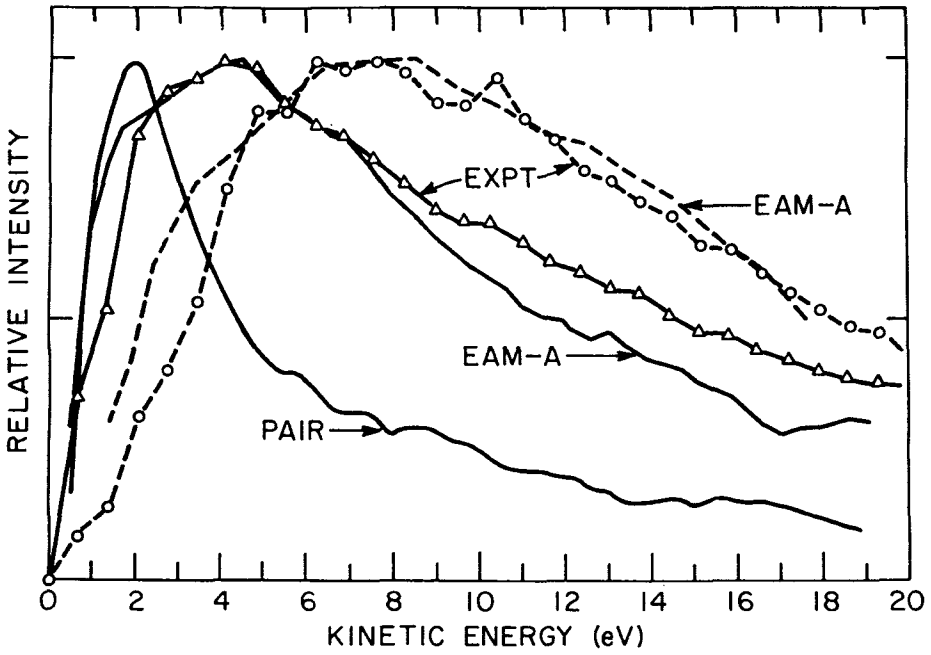

Figure 16. Experimental and calculated kinetic energy distributions. In all cases the curves are peak normalized. The two experimental curves are the angle-integrated distribution and one at $\phi = -30°$ and $\theta = 40 \pm 3°$. The EAM-M curves are the angle-integrated distribution and one at $\phi = -30°$ and $\theta = 38 \pm 7{\cdot}5°$. Only the angle-integrated distribution is shown for the pair-potential calculation. The angle-integrated distributions are shown as solid lines and the ones at $\phi \approx 40°$ are dashed lines. Reproduced with permission (Garrison *et al.* 1988).

4.2.8.3. *Epitaxy of metals on metals*

The epitaxy of metal atoms deposited on metal surfaces has undergone renewed activity, spurred on by the emergence of new technological advancements in monolayer deposition. The mechanisms of layer growth and the resulting structures are important in understanding the novel properties these systems display. The theoretical study of epitaxy has until recently focused on continuum models (Venables *et al.* 1984). If the deposited metal has a surface energy smaller than that of the substrate, it will tend to wet the surface, forming a single layer of atoms. In contrast, if the deposited metal has a higher surface energy, it will tend to form 3D clusters on the substrate.

We have already mentioned the inadequacy of pair potentials for describing surface phenomena. Accurate microscopic treatments are emerging with the development of the effective medium type methods and supercomputers. The CEM and MD/MC-CEM methods have been applied to the Rh on Ag(100) system (Raeker *et al.* 1990), motivated by the discovery (Schmitz *et al.* 1989) that when a deposited Rh film on Ag(100) is annealed to 600 K a sandwich-type structure was formed. In other words, an additional layer of Ag was formed on top of the original Rh layer which was on the Ag substrate. This effect was proposed to be due to the different surface energies of the two metals. Defects in the surface and adlayer were also assumed to enable Ag atoms to migrate from the substrate through the Rh layer and wet the Rh surface.

Prior to the dynamical calculations, interaction-energy calculations using both the CEM and MD/MC-CEM theories confirmed that a Rh layer is more stable under a Ag layer rather than exposed on the surface. Molecular-dynamics simulations were used in conjunction with the MD/MC-CEM forces to examine the initial evolution of the surface to subsurface chemisorption. These calculations suggested that the above proposed mechanism was essentially correct. Maximization of the Rh atom's binding energy drove the Rh to full coordination by exchanging position with a Ag surface atom. Once chemisorbed in a centre site, a Rh atom waited for the four nearest Ag surface atoms, oscillating in their lattice positions, to open a large enough gap to enable the Rh atom to displace a Ag atom. Once this process starts the Rh atoms had about an 80% success rate in completing the exchange.

It was observed that this exchange process catalysed itself at temperatures above 400 K. If there were a number of Rh atoms grouped together and one of them exchanged with a surface Ag atom, the others quickly followed. The exchange disturbed the surrounding Ag atoms enough to open gaps for the remaining nearby Rh atoms. The type of exchange spread until all the original surface Rh atoms in the cluster exchanged with the Ag. In contrast, if no atoms in a Rh cluster exchanged with Ag, the cluster maintained its original structure on the surface, indicating that diffusion of Rh on Ag played no role in the process. The amount of exchange was seen also to increase with temperature and the openness of the Ag surface (e.g. $(110) > (100) \gg (111)$).

If a defect-free ideal monolayer of Rh atoms were made and annealed (by computer simulation of course), it was found that no exchanges occurred for temperature as high as 1000 K. Removing a few random Rh atoms, and thereby creating defects, resulted in exchange that, once catalysed, would continue (if allowed to run long enough) until the supply of surface Rh adatoms was depleted. All these results implied that the formation of a sandwich compound was kinetically limited.

5. Extended EM-type theories

The applications in this review encompass a wide range of phenomena on pure metals, mixed metals and atoms interacting with these. They do not cover covalently bound molecules interacting with metals since these present severe problems for the present EM methods. The basic reason is easy to see within the CEM method, for example. To describe a molecule such as O_2, the covalent embedding function is required, while for O interacting with a metal surface the SCF-LD embedding function is appropriate. In the EM language, the one-electron energies for the molecule are extremely different from those of the atoms in jellium, while those of the chemisorbed atoms are quite similar to the atoms in jellium. Thus the corrections to the atom-in-jellium system are much larger in the former case. The end result is that a consistent description of the covalently bound molecule and the more ionically-bound atomic chemisorption is not provided. Since the energy balance between molecular bonds and atom–surface bonds is crucial in the description of the reaction, it is very difficult to describe the reaction correctly.

An empirical treatment of the molecule–surface interaction has been provided based upon use of a modified four-body LEPS form for the interaction of the molecule with the metal surface. This has been reviewed in great detail (DePristo 1989, DePristo and Kara 1990), so we just provide a brief outline here. The original idea of the four-body LEPS form was due to McCreery and Wolken (1977). This was later modified and quantified to be more accurate for metal surfaces by Lee and DePristo (1986) who

incorporated EM-like forms for the atom–surface interactions. Even more recently, Truong *et al.* (1989) have used EAM interactions for the atom–surface interactions.

For a diatomic molecule AB, interacting with a metal, M, the basic idea is to use valence-bond theory for the atom–surface interactions, V_{AM} and V_{BM}, along with V_{AB} to construct $V_{AB,M}$. The explicit form is

$$V_{AB,M}=Q_{AM}+Q_{BM}+Q_{AB}-[J_{AB}(J_{AB}-J_{AM}-J_{BM})+(J_{AM}+J_{BM})^2]^{1/2}, \tag{5.1}$$

where Q and J are Coulomb and exchange integrals respectively for each constituent. These are determined from the general forms

$$Q+J=V, \tag{5.2a}$$

$$Q-J=V^*, \tag{5.2b}$$

where V and V^* are the bonding and antibonding parts of the interactions respectively. The former are provided by a Morse potential for V_{AB} with EAM-like forms for V_{AM} and V_{BM}, which uses the SCF-LD embedding functions, electron density of the surface atoms and adjustable two-body potentials. The V^* are determined by arbitrary forms employing adjustable parameters, the so-called Sato parameters.

The important feature of this form is the non-additivity of the interaction potentials. It is the precise division into Q and J for each interaction in equation (5.1) that controls the topology and energies of the full molecule–surface interaction potential.

This empirical approach is only a temporary pragmatic solution. It does not address the problem of covalent *versus* ionic bonding in the effective-medium-type theories as described in the beginning of this section. Rather, it ignores the problem by not using the effective-medium-type theories for the covalently bonded moleclule. The price paid for this is the introduction of new arbitrary parameters to control the division into Coulomb and exchange interactions. These parameters must be determined for each molecule–surface combination.

A recent approach has attempted to interpolate the difference in one-electron energies within the EM method (Nørskov 1989). First, the known molecular binding potential was used to define the diatomic correction:

$$\delta_{\text{empty}}=\Delta E(A_1,A_2)-\sum_{i=1,2}\Delta E_{EM,i}(A_i;n_i). \tag{5.3}$$

Then SCF-LD calculations of the diatomic in jellium were used to define another correction δ_{filled}. Both these corrections depended upon the bond length of the molecule while δ_{filled} also depended upon the jellium electron density. The terminology, filled and empty, referred to the occupation of the lowest unoccupied molecular orbital (LUMO). The interpolation between the empty and filled correction was written as

$$\delta=n_{\text{LUMO}}\delta_{\text{filled}}+(1-n_{\text{LUMO}})\delta_{\text{empty}}, \tag{5.4}$$

where n_{LUMO} is the fractional occupation of the LUMO. This was determined from a tight-binding calculation. Initial results were very encouraging for the dissociative chemisorption of H_2 on the (100) (110) and (111) faces of Ni and Cu.

6. Discussion and summary

It is worthwhile to summarize the general capabilities and limitations of the current implementations of effective-medium-type theories. These methods can provide an

accurate description of metal–metal bonding for simple or transition metals with weak d bonding. This includes homogeneous and heterogeneous systems, and also extends to non-metallic binding of atoms to metals. All of the methods are less accurate for strong d bonding. They do not describe the difference in structural energies between different metallic coordinations at sufficient accuracy to distinguish among b.c.c., f.c.c. and h.c.p. structures. (The Finnis–Sinclair method uses a restriction to nearest neighbour interactions to overcome this problem, but this cannot be generalized to non-periodic structures.) Directional bonding is not incorporated consistently but must be incorporated by *a priori* specification of the electron density.

At present, the CEM method is the most general and applicable to small and large systems. It is also demanding enough computationally to limit its use to Monte Carlo simulations of systems with fewer than about 100 atoms. The EM method is also quite general and simpler computationally, but is restricted to more extended systems. Still simpler is the semi-empirical MD/MC-CEM method which eliminates kinetic-exchange-correlation energy inhomogeneity effects included in the CEM method, but which is also efficient enough computationally to be used in simulations on systems with many thousands of atoms. It can be applied to small and large systems but will be more accurate for the latter. For these three methods, the embedding energies depend only upon the type of atom and the jellium electron density. The two-body interactions are specified in terms of properties of the atoms (e.g. by the HF electron density in CEM) and are not adjustable. Changing the types of atoms does not entail any more difficulty in the calculation. These theories allow for predictions about a wide variety of heterogeneous systems.

The simplest methods are the EAM, Finnis–Sinclair and 'glue' models. Electron density, embedding and two-body functions are all determined empirically from experimental data. (In the 'glue' model an effective coordination function is defined rather than an electron density function.) Changing the atoms requires re-determination of the parameters. Some properties of heterogeneous systems must be used in order to predict others.

Implementation of these theories spans a wide range of computational difficulty. The empirical effective-medium-type methods are only slightly harder to apply than pair potentials. The MD/MC-CEM method is considerably more difficult, requiring HF densities and embedding functions, and routines for overlap integrals, Coulomb integrals and Chebyshev smoothing. The CEM theory also requires multicentre numerical integration.

The development of these methods over the past decade has led to a multitude of applications which were essentially comparisons between experiment and theory to test the accuracy of the latter. Now, with an understanding of the adequacies and inadequacies of the various theories, we expect more significant applications to predictions of chemical, mechanical and dynamical properties of metallic systems.

Acknowledgments

Ames Laboratory is operated for the U.S.A. Department of Energy by Iowa State University under contract No. W-7405-Eng-82. This article was supported in part by the Division of Chemical Sciences, Office of Basic Energy Sciences. This article also has been supported in part by the National Science Foundation, division of Chemical Physics.

References

ABRAMOWITZ, M., and STEGUN, I. A., 1972, *Handbook of Mathematical Functions* (New York: Dover).

ADAMS, D. L., PETERSEN, L. E., and SORENSEN, C. S., 1985, *J. Phys.* C, **18,** 1753.

ADAMS, J. B., and WOLFER, W. G., 1988, *J. nucl. Mater.*, **158,** 25.

ANDERSON, J. N., NIELSON, H. B., PETERSON, L., and ADAMS, D. L., 1984, *J. Phys.* C, **17,** 173.

ANDREA, T. A., SWOPE, W. C., and ANDERSEN, H. C., 1983, *J. chem. Phys.*, **79,** 4576.

AVOURIS, PH., KAWAI, R., LANG, N. D., and NEWNS, D. M., 1988, *J. chem. Phys.*, **89,** 2388.

BADDORF, A. B., LYO, I. W., PLUMMER, E. W., and DAVIS, H. L., 1987, *J. Vac. Sci. Technol.* A, **5,** 782.

BAGUS, P. S., GILBERT, T. L., and ROOTHAN, C. J., 1972, *J. chem. Phys.*, **56,** 5195.

BASKES, M. I., 1984, *J. nucl. Mater.*, **128–129,** 676; 1987, *Phys. Rev. Lett.*, **59,** 2666.

BASKES, M. I., FOILES, S. M., and MELIUS, C. F., 1987, *J. nucl. Mater.*, **145,** 339.

BASKES, M. I., FOILES, S. M., and DAW, M. S., 1988, *J. Phys., Paris,* C5–483.

BASKES, M. I., NELSON, J. S., and WRIGHT, A. F., 1989, *Phys. Rev.* B, **40,** 6085.

BATALLA, E., STROM-OLSEN, J. D., ALTOUNIAN, Z., BOOTHROYD, D., and HARRIS, R., 1986, *J. Mater. Res.*, **1,** 765.

BECKE, A. D., 1986, *J. chem. Phys.*, **84,** 4524; 1988, *Ibid.*, **88,** 2547.

BESENBACHER, F., NIELSEN, B. B., MYERS, S. M., 1984, *J. appl. Phys.*, **56,** 3384.

BESENBACHER, F., MYERS, S. M., NORDLANDER, P., and NOERSKOV, J. K., 1987, *J. appl. Phys.*, **61,** 1788.

BIANCONI, A., and BACHRACH, R. Z., 1974, *Phys. Rev. Lett.*, **42,** 104.

BRONGERSMA, H. H., SPARNAY, M. J., and BUCK, T. M., 1981, *Surf. Sci.*, **71,** 657.

CARNEVALI, P., ERCOLESSI, F., TOSATTI, E., 1987, *Surf. Sci.*, **189–190,** 645.

CHAKRABORTY, B., HOLLOWAY, S., and NØRSKOV, J. K., 1985, *Surf. Sci.*, **152/53,** 660.

CHAN, C. M., and VAN HOVE, M. A., 1986, *Surf. Sci.*, **171,** 226.

CHELIKOWSKY, J. R., 1984, *Surf. Sci.*, **139,** L197.

CHEN, S. P., VOTER, A. F., and SROLOVITZ, D. J., 1986, *Phys. Rev. Lett.*, **57,** 1308.

CHEN, S. P., SROLOVITZ, D. J., and VOTER, A. F., 1989, *J. Mater. Res.*, **4,** 62.

CLEMENTI, E., 1965, *IBM J. Res. Develop. Suppl.*, **9.**

COPEL, M., and GUSTAFSSON, T., 1986, *Phys. Rev. Lett.*, **57,** 723.

DAW, M. S., BISSON, C. L., and WILSON, W. D., 1983, *Solid-St. Commun.*, **46,** 735.

DAW, M. S., and BASKES, M. I., 1984, *Phys. Rev.* B, **29,** 6443.

DAW, M. S., and HATCHER, R. D., 1985, *Solid-St. Commun.*, **56,** 697.

DAW, M. S., 1986, *Surf. Sci.*, **166,** L161; 1989, *Phys. Rev.* B, **39,** 7441.

DAW, M. S., and FOILES, S. M., 1987a, *Phys. Rev. Lett.*, **59,** 2756; 1987b, *Phys. Rev.* B, **35,** 2128.

DELLEY, B., 1990, *J. chem. Phys.*, **92,** 508.

DEMUTH, J. E., MARCUS, P. M., and JEPSEN, D. W., 1975, *Phys. Rev.* B, **11,** 1460.

DEPRISTO, A. E., and KRESS, J. D., 1987a, *Phys. Rev.* A, **35,** 438; 1987b, *J. chem. Phys.*, **86,** 1425.

DEPRISTO, A. E., 1989, *Interactions of Atoms and Molucules with Solid Surfaces,* edited by A. Bortolani, N. March and M. Tosi (New York: Plenum).

DEPRISTO, A. E., and KARA, A., 1990, *Adv. chem. Phys.*, **77.**

DIRAC, P. A. M., 1930, *Proc. Camb. phil. Soc.*, **26,** 376.

DODSON, B. W., 1987a, *Phys. Rev.* B, **35,** 880; 1987b, *Phys. Rev.* B, **36,** 6288; 1987c, *Surf. Sci.*, **184,** 1; 1988, *Phys. Rev. Lett.*, **60,** 2288.

DONDI, M. G., TERRENI, S., TOMMASINI, F., and LINKE, U., 1988, *Phys. Rev. B,* **37,** 8034.

EGELHOFF, W. R., JR, 1983, *Phys. Rev. Lett.*, **50,** 587; 1984, *Phys. Rev.* B, **30,** 1052.

ERCOLESSI, F., PARRINELLO. M., and TOSATTI, E., 1986, *Surf. Sci.*, **177,** 314; 1988, *Phil. Mag.* A, **58,** 213.

ERCOLESSI, F., BARTOLINI, A., GAROFALO, M., PARRINELLO, M., and TOSATTI, E., 1987a, *Surf. Sci.*, **189–190,** 636; 1987b, *Phys. Scripta.* B, **T19,** 399.

FELTER, T. E., FOILES, S. M., DAW, M. S., and STULEN, R. H., 1986, *Surf. Sci.*, **171,** L379.

FINNIS, M. W., and SINCLAIR, J. E., 1984, *Phil. Mag.* A, **50,** 45.

FINNIS, M. W., PAXTON, A. T., PETTIFOR, D. G., SUTTON, A. P., and OHTA, Y., 1988, *Phil. Mag.* A, **58,** 143.

FOILES, S. M., 1985a, *Phys. Rev.* B, **32,** 7685; 1985b, *Ibid.*, **32,** 3409; 1987a, *Mater. Res. Soc. Symp. Proc.*, **83,** 175; 1987b, *Ibid.*, **81,** 51; 1987c, *Surf. Sci.*, **191,** L779; 1987d, *Ibid.*, **191,** 329.

FOILES, S. M., BASKES, M. I., and DAW, M. S., 1986, *Phys. Rev.* B, **33,** 7983; 1988, *Mater. Res. Soc. Symp. Proc.*, **122,** 343; 1989, *Mater. Sci. Forum,* **37,** 223.

FOILES, S. M., and DAW, M. S., 1987, *J. Mater. Res.*, **2,** 5.
FOILES, S. M., BASKES, M. I., MELIUS, C. F., and DAW, M. S., 1987, *J. less-common Metals*, **130,** 465.
FOILES, S. M., and ADAMS, J. B., 1989, *Phys. Rev.* B, **40,** 5909.
FRENKEN, J. W. M., and VAN DER VEEN, J. F., 1985, *Phys. Rev. Lett.*, **54,** 134.
FRENKEN, J. W. M., VAN DER VEEN, J. F., and ALLAN, G., 1983, *Phys. Rev. Lett.*, **51,** 1876.
FRIGO, A., TOIGO, F., COLE M. W., and GOODMAN, F. O., 1986, *Phys. Rev.* B, **33,** 4184.
FRÖYEN, S., HOLLOWAY, S., NØRSKOV, J. K., and CHAKRABORTY, B., 1986, *J. Electron Spectrosc.*, **38,** 313.
GAROFALO, M., TOSATTI, E., and ERCOLESSI, F., 1987, *Surf. Sci.*, **188,** 321.
GARRISON, B. J., WINOGRAD, N., DEAVEN, D. M., REIMANN, C. T., LO, D. Y., TOMBRELLO, T. A., HARRISON, JR. D. E., and SHAPIRO, M. H., 1988, *Phys. Rev.* B, **37,** 7197.
GAUTHIER, Y., BAUDOING, R., LUNDBERG, M., and RUNDGREN, J., 1987, *Phys. Rev.* B, **35,** 7867.
GHOSH, S. K., and PARR, R. G., 1986, *Phys. Rev.* A, **34,** 785.
GILMORE, C. M., SPRAGUE, J. A., ERIDON, J. M., and PROVENZANO, V., 1989, *Surf. Sci.*, **218,** 26.
GORDON, R. G., and KIM, Y. S., 1972, *J. chem. Phys.*, **56,** 3122.
GUNNARSSON, O., and LUNDQVIST, B. I., 1976, *Phys. Rev.* B, **13,** 4274.
HO, K. M., and BOHNEN, K. P., 1985, *Phys. Rev.* B, **32,** 3446.
HOLMBERG, C., FONDEN, T., MAELLO, A., and LUNDQVIST, B. I., 1987, *Phys. Scripta*, **35,** 181.
HOTOP, H., and LINEBERGER, W. C., 1975, *J. Phys. chem. Ref. Data*, **4,** 539.
HUZINAGA, S., 1967, *Prog. theor. Physics Suppl.*, **40,** 279.
JACOBSEN, K. W., and NØRSKOV, J. K., 1986, *Surf. Sci.*, **166,** 539; 1987, *Phys. Rev. Lett.*, **59,** 2764; 1988, *Ibid.*, **60,** 2496.
JACOBSEN, K. W., NØRSKOV, J. K., and PUSKA, M. J., 1987, *Phys. Rev.* B, **35,** 7423.
JACOBSEN, K. W., 1988, *Comments condens. Matter Phys.*, **14,** 129.
JENA, P., NIEMINEN, R. M., PUSKA, M. J., and MANNINEN, M., 1985, *Phys. Rev.* B, **31,** 7612.
KARA, A., and DEPRISTO, A. E., 1988, *Surf. Sci.*, **193,** 437.
KARIKORPI, M., HOLLOWAY, S., HENRIKSEN, N., and NØRSKOV, J. K., 1987, *Surf. Sci.*, **179,** L41.
KARIMI, M., and VIDALI, G., 1987, *Phys. Rev.* B, **36,** 7576; 1988, *Ibid.*, **38,** 7759; 1989, *Surf. Sci.*, **208,** L73.
KIM, Y. S., and GORDON, R. G., 1974, *J. chem. Phys.*, **60,** 1842.
KITTEL, C., 1971, *Introduction to Solid State Physics* (New York: John Wiley).
KRESS, J. D., and DEPRISTO, A. E., 1987, *J. chem. Phys.*, **87,** 4700; 1988, *Ibid.*, **88,** 2596.
KRESS, J. D., STAVE, M. S., and DEPRISTO, A. E., 1989, *J. Phys. Chem.*, **93,** 1556.
LEE, C. Y., and DEPRISTO, A. E., 1986, *J. chem. Phys.*, **85,** 4161; 1987a, *J. Vac. Sci. Technol.* A, **85,** 485; 1987b. *J. chem. Phys.*, **87,** 1401.
LUNDBERG, M., 1987, *Phys. Rev.* B, **36,** 4692.
LUNDQVIST, B. I., FONDEN, T., IDIODI, J., JOHNSSON, P., MAALLO, A., and PAPADIA, S., 1987, *Prog. Surf. Sci.*, **25,** 191.
MAARLEVELD, P. R., KAARS, P. B., WEEBER, A. W., and BAKKER, H., 1986, *Physica* B + C, **142,** 328.
MANNINEN, M., NØRSKOV, J. K., and UMRIGAR, C., 1982, *Surf. Sci.*, **119,** L393.
MANNINEN, M., PUSKA, M. J., NIEMINEN, R. M., and JENA, P., 1984, *Phys. Rev.* B, **30,** 1065.
MCCREERY, J. H., and WOLKEN, G., 1977, *J. chem. Phys.*, **67,** 2551.
MCMULLEN, T., STOTT, M. J., and ZAREMBA, E., 1987, *Phys. Rev.* B, **35,** 1076.
MCMULLEN, T., PLUMER, M. L., STOTT, M. J., and ZAREMBA, E., 1988, *Phys. Rev.* B, **38,** 1077.
MIEDEMA, A. R., 1978, *Z. Metallk.*, **69,** 455.
MORITZ, W., and WOLF, D., 1985, *Surf. Sci.*, **163,** L655.
MORSE, M. D., 1986, *Chem. Rev.*, **86,** 1049.
MUHLHAUSEN, C., and GORDON, R. G., 1981, *Phys. Rev.* B, **23,** 900.
MUKERJEE, S., and MORAN-LOPEZ, J. L., 1987, *Surf. Sci.*, **188,** L742.
MYERS, S. M., BESENBACHER, F., and NØRSKOV, J. K., 1985a, *J. appl. Phys.*, **58,** 1841.
MYERS, S. M., WAMPLER, W. R., BESENBACHER, F., ROBINSON, S. L., and MOODY, N. R., 1985b, *Mater. Sci. Engng*, **69,** 397.
MYERS, S. M., NORDLANDER, P., BESENBACHER, F., and NOERSKOV, J. K., 1986, *Phys. Rev.* B, **33,** 854.
MYERS, S. M., RICHARDS, P. M., WAMPLER, W. R., and BESENBACHER, F., 1989, *J. nucl. Mater.*, **165,** 9.
NELSON, J. S., SOWA, E. C., and DAW, M. S., 1988, *Phys. Rev. Lett.*, **61,** 1977.
NG, Y. S., TSONG, T. T., and MCLANE, JR, S. B., 1979, *Phys. Rev. Lett.*, **42,** 588.

NIELSEN, B. B., VAN VEEN, A., 1985, *J. Phys.* F, **15,** 2409.
NINGSHENG, L., WENLAN, X., and SHEN, S. C., 1988a, *Solid-St. Commun.*, **67,** 837; 1988b, *Phys. Stat. sol. (b)*, **147,** 511; 1989, *Solid-St. Commun.*, **69,** 155.
NOONAN, J. R., and DAVIS, H. L., 1990, *J. Vac. Sci. Technol.* A (submitted).
NORDLANDER, P., NØRSKOV, J. K., and BESENBACHER, F., 1986, *J. Phys.* F, **16,** 1161.
NØRSKOV, J. K., and LANG, N. D., 1980, *Phys. Rev.* B, **21,** 2131.
NØRSKOV, J. K., 1982, *Phys. Rev. Lett.*, **48,** 1620; 1984, *Physica* B+C, **127,** 193; 1989, *J. chem. Phys.*, **90,** 7461.
NØRSKOV, J. K., and BESENBACHER, F., 1987, *J. less-common Metals*, **130,** 475.
OSSI, P. M., 1988, *Surf. Sci.*, **201,** L519.
PLUIS, B., DERNIER VAN DER GON, A. W., FRENKEN, J. W. M., and VAN DER VEEN, J. F., 1987, *Phys. Rev. Lett.*, **59,** 2678.
PERDEW, J. P., and YUE, W., 1986, *Phys. Rev.* B, **33,** 8800.
PERDEW, J. P., 1986, *Phys. Rev.* B, **33,** 8822.
PUSKA, M. J., NIEMINEN, R. M., and JENA, P., 1987, *Phys. Rev.* B, **35,** 6059.
PUSKA, M. J., NIEMINEN, R. M., and MANNINEN, M., 1981, *Phys. Rev.* B, **24,** 3037.
RAEKER, T. J., and DEPRISTO, A. E., 1989, *Phys. Rev.* B, **39,** 9967; 1990, *Surf. Sci* (to be published).
RAEKER, T. J., and DEPRISTO, A. E., 1990, *Scanning Microscopy International* (submitted).
RAEKER, T. J., SANDERS, D. E., and DEPRISTO, A. E., 1990, *J. Vac. Sci. Technol.* A (to be published).
RAO, B. K., JENA, P., SCHILLADY, D. D., HINTERMANN, A., and MANNINEN, M., 1985, *Solid-St. Commun.*, **55,** 725.
REDFIELD, A. C., and ZANGWILL, A., 1987, *Phys. Rev. Lett.*, **58,** 2322.
RONAY, M., and NORLANDER, P., 1988, *Physica* C, **153–155,** 834.
ROSE, J. H., FERRANTE, J., and SMITH, J. R., 1981, *Phys. Rev. Lett.*, **47,** 675.
SALAHUB, D. R., and ZERNER, M. C., 1989, *The Challenge of d and f Electrons: Theory and Computation* (American Chemical Society).
SANDERS, D. E., STAVE, M. S., and DEPRISTO, A. E., 1990, *J. comput. Phys.* (submitted).
SCHMIDT, M. W., and RUEDENBERG, K. J., 1979, *Chem. Phys.*, **71,** 3951.
SINNOTT, S. B., RAEKER, T. J., and DEPRISTO, A. E., 1990, *Surf. Sci.* (submitted).
STAVE, M. S., SANDERS, D. E., RAEKER, T. J., and DEPRISTO, A. E., 1990, *J. chem. Phys.* (submitted).
STAVE, M. S., and DEPRISTO, A. E., 1990 (to be published).
STEIGERWALD, D. A., and WYNBLATT, P., 1988, *Surf. Sci.*, **193,** 287.
STOLTZE, P., JACOBSEN, K. W., and NØRSKOV, J. K., 1987, *Phys. Rev.* B, **36,** 5035.
STOLTZE, P., NØRSKOV, J. K., and LANDMAN, U., 1988, *Phys. Rev. Lett.*, **61,** 440.
STROUD, A. H., and SECREST, D., 1966, *Gaussian Quadrature Formulas* (New York: Prentice Hall).
STOTT, M. J., and ZAREMBA, E., 1980, *Phys. Rev.* B, **22,** 1564.
TOIGO, F., and COLE, M. W., 1985, *Phys. Rev.* B, **32,** 6989.
TORRENS, I. M., 1972, *Interatomic Potentials* (New York: Academic).
TING, N., QINGLIANG, Y., and YIYING, Y., 1988, *Surf. Sci.*, **206,** L857.
TRUONG, T. N., TRUHLAR, D. G., and GARRETT, B. C., 1990, *J. phys. Chem.* (to be published).
UNDERHILL, P. R., 1988, *Surf. Sci.*, **195,** 557.
VENABLES, J. A., SPILLER, G. D. T., and HANDBUCKEN, M., 1984, *Rep. Prog. Phys.*, **47,** 399, and references therein.
VIDALI, G., HUTCHINGS, C. W., and KARIMI, M., 1988, *Surf. Sci.*, **202,** L595.
VIDALI, G., and KARIMI, M., 1989, *Langmuir*, **5,** 612.
VON BLACKENHAGEN, P., SCHOMMERS, W., and VOEGELE, V., 1987, *J. Vac. Sci. Technol.* A, **5,** 649.
VOTER, A. F., 1988, *Proc. SPIE*, **821,** 214.
WALDMAN, M., and GORDON, R. G., 1979, *J. chem. Phys.*, **71,** 1325.
WEBBER, R., ROJAS, C. E., DOBSON, P. J., and CHADWICK, D., 1981, *Surf. Sci.*, **105,** 20.
WOLFER, W. G., VAN SICLEN, C. D., FOILES, S. M., and ADAMS, J. B., 1989, *Acta metall*, **37,** 579.
TYSON, W. R., and MILLER, W. A., 1977, *Surf. Sci.*, **62,** 267.
ZANGWILL, A., 1988, *Physics at Surfaces* (Cambridge University Press).